Late Cenozoic shortening in the west-central Alborz Mountains, northern Iran, by combined conjugate strike-slip and thin-skinned deformation

Bernard Guest*
Gary J. Axen*
Patrick S. Lam
Department of Earth and Space Sciences, University of California, Los Angeles, California 90095-1567, USA

Jamshid Hassanzadeh
Department of Geology, University of Tehran, Tehran, Iran

ABSTRACT

The west-central Alborz Mountains of northern Iran have deformed in response to the Arabia-Eurasia collision since ca. 12 Ma and have accommodated 53 ± 3 km of shortening by a combination of range-parallel, conjugate strike-slip faulting and range-normal thrusting. By our interpretation, ~17 km of shortening across the Alborz is accommodated by westward relative motion of a crustal wedge bounded by conjugate dextral and sinistral strike-slip fault systems. The Nusha, Barir, and Tang-e-Galu fault zones strike west-northwest, constrain the north side of the wedge, and, prior to ca. 5 Ma, accumulated a total of ~25 km of dextral slip. The south side of the wedge is bounded by the active sinistral reverse Mosha and Taleghan faults, which merge northwest of Tehran and have a total slip estimate of 30–35 km. A restored cross section across the range indicates a minimum of 36 ± 2 km of fold-and-thrust–related, range-normal shortening. Combined, wedge motion, thrusting, and folding yield a net shortening of 53 ± 3 km across the range, which is within the error of the shortening estimate predicted by assuming that the present-day shortening rate (5 ± 2 mm/yr) has been constant since ca. 12 Ma (~60 km of predicted shortening). A second restored cross section farther west, which includes the wedge, gives a total shortening of 15–18 km and a long-term shortening rate of 1.25–1.5 mm/yr (constant shortening rate since ca. 12 Ma). These strong along-strike finite-strain and long-term strain-rate gradients are important for our understanding of how long-term strain rates compare with instantaneous strain rates derived from global positioning system (GPS) data, and should be considered when planning mountain belt–scale GPS surveys. Finally, a 60-km-long right-hand bend in the Mosha-Taleghan fault system has driven the development of a transpressional duplex south of the fault. The southern boundary of the duplex is the active Farahzad–Karaj–North Tehran thrust system. The kinematic development of this strike-slip duplex has implications for seismic hazard assessment in the heavily populated Karaj and Tehran areas.

Keywords: Iran, shortening, collision, Alborz, seismic hazard.

INTRODUCTION

The architecture, kinematics, and structural evolution of the Alborz Mountains (Fig. 1) are poorly understood and are relevant to understanding the mechanism that supports the isostatically undercompensated Alborz topography (peak heights of 3–5 km above an ~35–40-km-thick crust; Dehghani and Makris, 1984) and the mechanism driving rapid post–6 Ma subsidence in the south Caspian basin (~25 km of post-Jurassic sediment). The structural architecture of the Alborz remains controversial. Maps at 1:250,000 scale show an upward-diverging set of thrusts (Annells et al., 1975b, 1977; Huber and Eftekhar-nezhad, 1978a, 1978b; Vahdati Daneshmand, 1991). Stocklin (1974a) completed the first detailed cross sections across the Alborz, which were later expanded upon by Huber and Eftekhar-nezhad (1978a, 1978b) and adapted by Şengör (1990) to show the range as a transpressional, south-vergent flower structure. Axen et al. (2001b) noted that several of the "thrusts" have normal separations and interpreted the assemblage as an asymmetrical, south-vergent, transpressional flower structure. Similarly, Jackson et al. (2002) and Allen et al. (2003) considered the Alborz to be a sinistral transpressional belt, where slip is partitioned between sinistral strike-slip faults and thrust faults. Alavi (1996) interpreted the Alborz as a thin-skinned fold-and-thrust belt that has "formed a complex composite antiformal stack," which is cut by detachment and normal faults that drop the south Caspian down relative to the Alborz. This implies southward thrusting of the Alborz over central Iran, extensional subsidence along the southern margin of the south Caspian basin, and extensional collapse of the Alborz "composite antiformal stack."

These contrasting interpretations of the Alborz structure suggest markedly different geodynamic processes acting in northern Iran. For example, the symmetrical transpressional flower structure model for the Alborz (e.g., Allen et al., 2003) is consistent with the idea that flexural support for the Alborz may be provided by underthrust south Caspian oceanic (?) crust (as initially suggested by Axen et al., 2001a). On the other hand, the south-vergent asymmetrical flower structure geometry (e.g., Şengör, 1990) is consistent with a wedge of buoyant continental crust being driven beneath the Alborz from the south (e.g., Axen et al., 2001b). Alternatively, the Alavi (1996) orogenic collapse model implies that the Alborz structure is resting on weak, ductile middle or lower crust. This is consistent with the idea that lower-middle crustal channel flow from beneath the Turkish-Iranian plateau and Zagros Mountains may dynamically support the Alborz, as material moving around the subsided, rigid Caspian block slows and accumulates along the margins of the block.

*Current address: Guest—Institute of Geologie, University of Hannover, Hannover, Germany; Axen—New Mexico School of Mines and Engineering, Socorro, New Mexico, USA

Geosphere; February; v. 2; no. 1; p. 35–52; doi: 10.1130/GES00019.1; 12 figures; 3 plates.

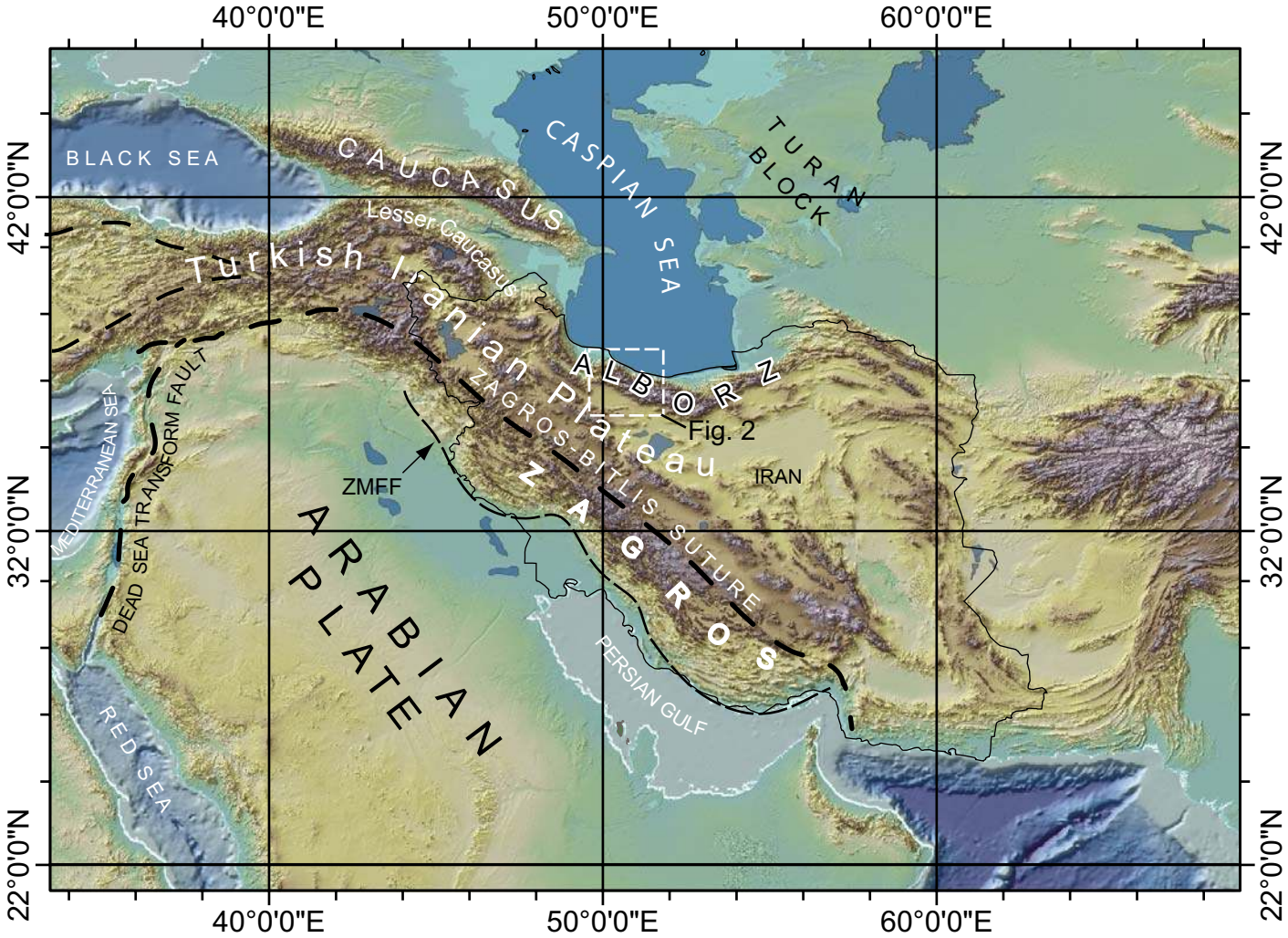

Figure 1. Shaded relief map showing the Arabia-Eurasia collision zone. Iran's border is shown in black. Labels refer to major physiographic and tectonic units. ZMFF—Zagros Mountain front flexure. The box over the western Alborz Mountains shows the location and coverage of Figure 2.

Another problem with our understanding of this range is that there is a mismatch between the finite shortening estimate across the range (30–35 km; Allen et al., 2003), the estimate for the onset of mountain building and deformation (ca. 12 Ma; Guest, 2004), and the 5 ± 2 mm/yr range-perpendicular global positioning system (GPS) shortening rate (Vernant et al., 2004). Assuming a constant time-averaged shortening rate of ~5 mm/yr over ~12 m.y. gives a total finite shortening of ~60 km, which is twice the current estimate.

To improve our understanding of the structural architecture and the spatial and temporal distribution of late Cenozoic deformation in the Alborz, we present a mapped transect across the western Alborz compiled from our detailed geological mapping, satellite image interpretation, and maps from Ph.D. theses and the Iranian Geological Survey (Plates 1, 2, and 3). We include data from the major fault systems in the western Alborz (Fig. 2), as well as a restored structural cross section (Plate 2). Our interpretation of the west-central Alborz structure is similar to the interpretations of Stocklin (1974a), Huber and Eftekhar-nezhad, (1978a, 1978b), and Şengör (1990), and is consistent with finite sinistral-transpressional shortening of 53 ± 3 km across the range and a south-vergent asymmetrical flower structure cross-sectional geometry.

GEOTECTONIC SETTING

Geologic History

The Alborz and adjacent central Iranian crust are considered to be parts of a fragment of the early Paleozoic Gondwanan passive margin that rifted away from Gondwana during Ordovician to Silurian time and collided with Eurasia during Triassic time (Stocklin, 1974b; Berberian and King, 1981; Şengör et al., 1988; Şengör, 1990; Stampfli et al., 1991; Şengör and Natal'in, 1996). The suture between northern Iran and Eurasia is thought to lie along the northern foot of the Alborz, where it is depositionally overlapped by >1 km of the Jurassic Shemshak Formation (Assereto, 1966; Stocklin, 1974a, 1974b; Stocklin and Setudehnia, 1977; Berberian and Berberian, 1981; Berberian, 1983; Şengör, 1990; Şengör and Natal'in, 1996) (Fig. 2; Plate 1).

A late Cretaceous to Paleocene compressional event that occurred along the Neotethyan margin is represented in the Alborz by a sequence of folded and faulted Cretaceous to Paleocene marine carbonate, clastic, and volcanic rocks, which conformably overlie the

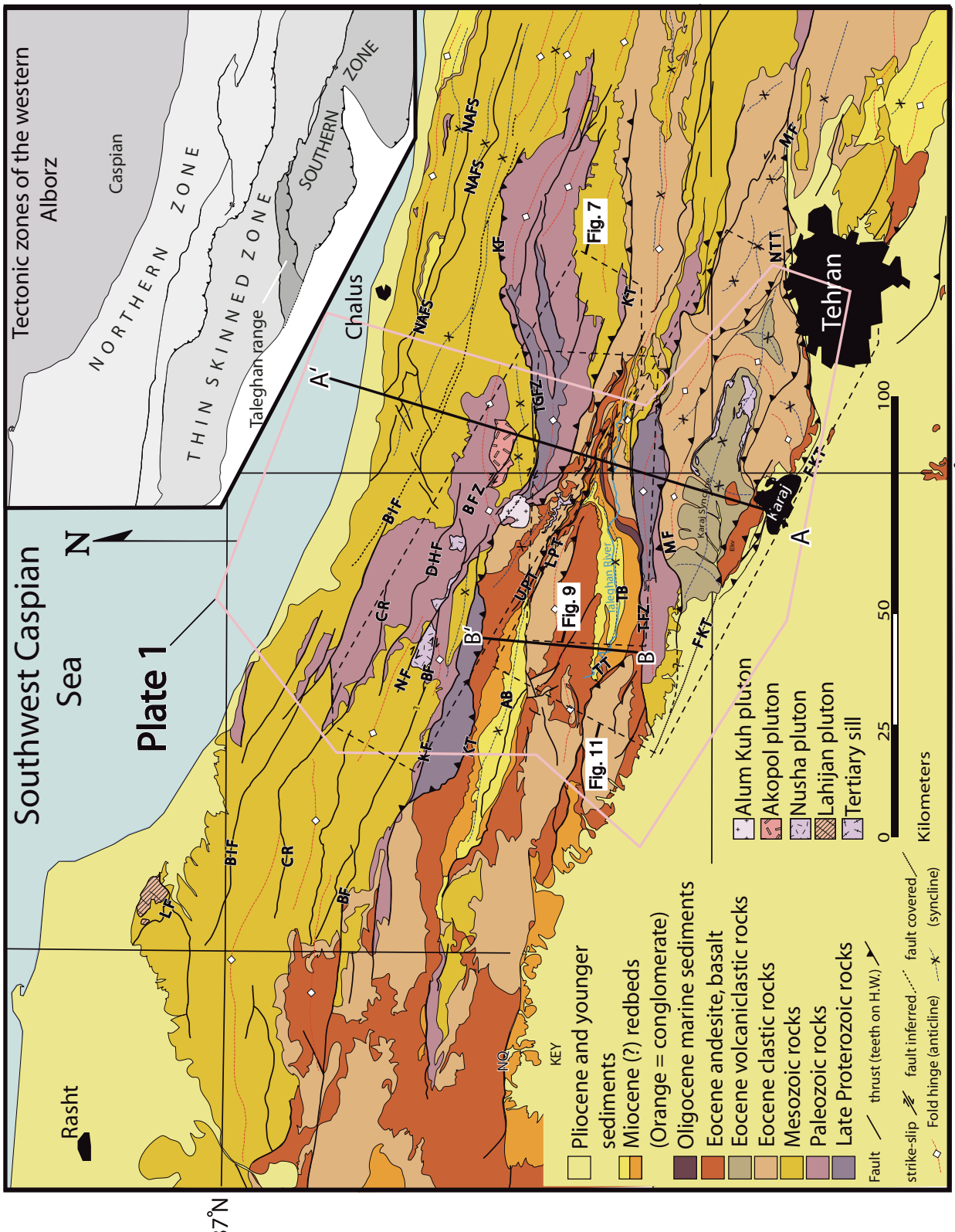

Figure 2. Map showing regional geology of the western Alborz. Insets show Alborz structural zones. Dashed rectangles show locations of maps in later figures. BF—Banan fault; BFZ—Barir fault zone; BIF—Binaksar fault; CR—Chalk Rud fault; DHF—Doh Hezar fault (informal name); KF—Khashachal fault; KT—Kandavan thrust; LF—Lahijan fault; LPT—lower Parachan thrust; MFT—Mosha Fasham thrust; NAFS—north Alborz fault system; NQ—north Qazvin fault; NTT—North Tehran thrust; NF—Nusha fault; TGFZ—Tang-e-Galu fault zone; TT—Takieh thrust; TFZ—Taleghan fault zone; UPT—upper Parachan thrust; TB—Taleghan Basin; AB—Alamut basin.

Shemshak Formation and underlie transgressive early to middle Eocene carbonates and volcanic rocks that do not show evidence of syncontractional deposition (Stocklin, 1974a; Stocklin and Setudehnia, 1977) (Figs. 2 and 3; Plates 1, 2, and 3).

The early to middle Eocene Karaj Formation volcanic and volcaniclastic rocks unconformably overlie the older deformed sequences and are widely exposed in the southern Alborz. The Karaj Formation shows evidence of synextensional deposition and is interpreted to record backarc extension and subsidence in northern Iran during early to middle, and possibly late(?), Eocene time (Berberian, 1983; Hassanzadeh et al., 2002; Allen et al., 2003). In the south-central Alborz, the Karaj Formation is unconformably overlain by a sequence of Oligocene-Miocene volcanics and marine carbonates, which are, in turn, erosionally truncated and unconformably overlain by middle to late Miocene conglomeratic growth strata, which probably correlate with the onset of rapid uplift and denudation at ca. 12 Ma (Guest, 2004).

The ca. 12 Ma onset of rapid denudation is based on apatite and zircon U-Th/He and K-feldspar Ar/Ar cooling ages from samples of the Nusha and Akapol plutons, located in the high central Alborz (Fig. 2). These data indicate an increase in denudation rate from ~0.1 km/m.y. as late as 12 Ma to ~0.45 km/m.y. since ca. 12 Ma. This estimate for the onset of rapid exhumation agrees well with some estimates for the onset of the Arabia-Eurasia collision (e.g., McQuarrie et al., 2003).

A late middle Miocene or Serravallian age for the onset of Arabia-Eurasia collision is supported by several lines of evidence: (1) the switch from marine to syncontractional alluvial and fluvial deposition during the middle to late Miocene in the Alborz (Guest, 2004), (2) onset of rapid exhumation of the Nusha pluton in the west-central Alborz at ca. 12 Ma (Guest, 2004), (3) rapid exhumation of the Akapol and Alam Kuh plutons in the west-central Alborz during late Miocene time (Axen et al., 2001a), (4) plate-circuit rotations and crustal shortening estimates that show closure of the Neotethys no later than 10 Ma (McQuarrie et al., 2003), (5) development of widespread unconformities across the present Turkish-Iranian plateau during middle to late Miocene time (Dewey and Şengör, 1979; Şengör and Kidd, 1979), (6) deformation of early to middle Miocene intercontinental flysch deposits in southeastern Anatolia (Yilmaz, 1993), and (7) closure of the Neotethyan ocean basin at ca. 14 Ma, determined from carbon and oxygen isotope analysis of benthic foraminifera, which show that warm salty water known as Tethyan/Indian saline water was flowing into the Indian Ocean from the Tethys Ocean up until 14 Ma, after which time, circulation patterns shifted to the present thermohaline circulation system (Woodruff and Savin, 1989; Mohajjel et al., 2003).

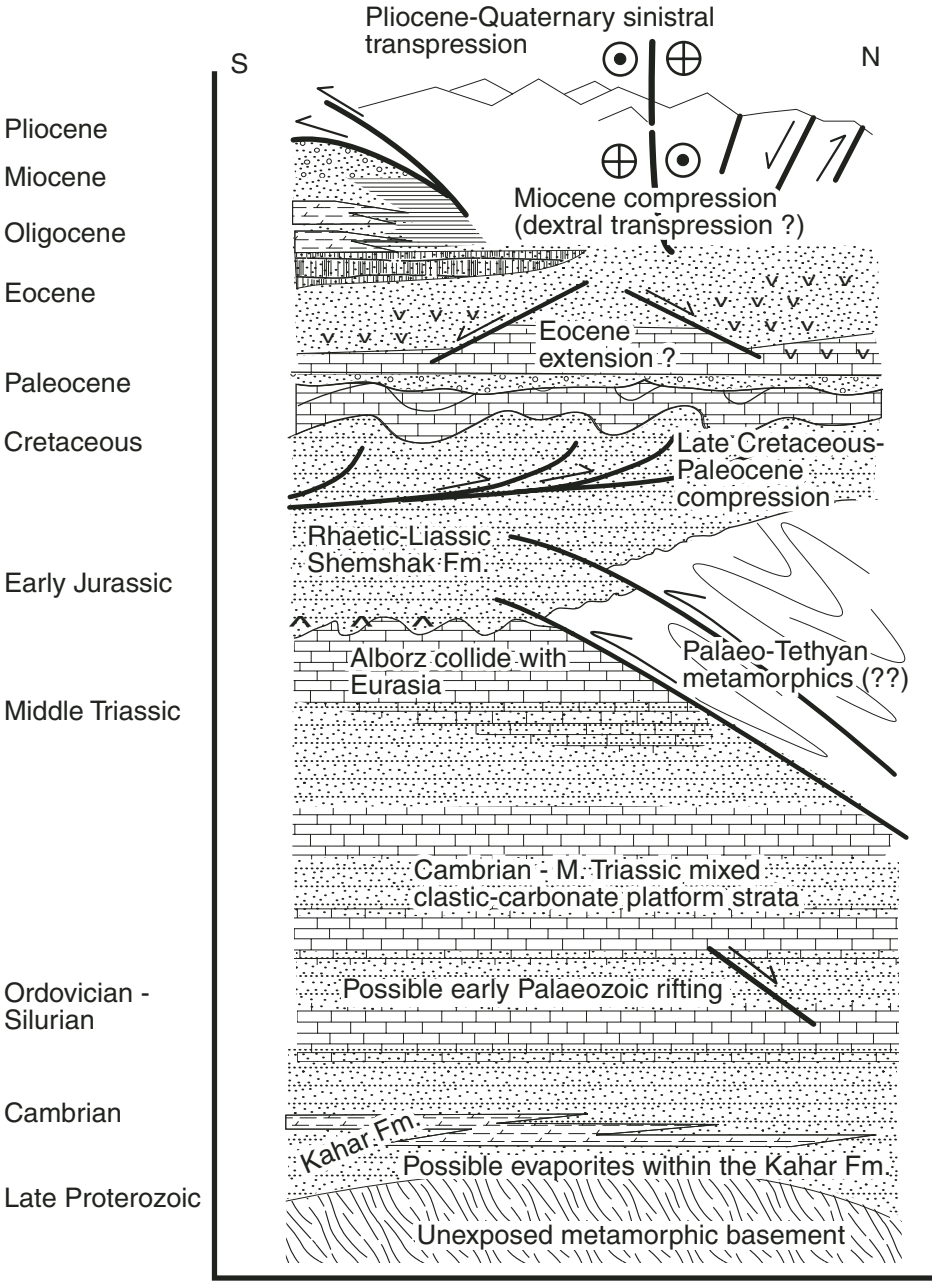

Figure 3. Schematic tectonostratigraphy of the Alborz, modified from Allen et al. (2003) by including Cretaceous deformational event.

Shortening Amounts and Rates

Total shortening across the Arabia-Eurasia collision zone is ~150 km. Of this, 57–87 km is accommodated in the Zagros Mountains (McQuarrie, 2004), and ~75 km is accommodated in the Kopet Dagh fold-and-thrust belt (Lyberis and Manby, 1999). The best estimate for total shortening across the Alborz is 30 km (Allen et al., 2003).

The Arabia-Eurasia convergence rate is based on campaign GPS studies, which indicate ~16–22 mm/yr north to north-northeast convergence. Internal shortening in the Zagros accounts for 3 ± 2 to 8 ± 2 mm/yr, central Alborz accounts for 5 ± 2 mm/yr, the eastern Alborz and Kopet

Dagh account for 14 ± 2 mm/yr, and central Iran (south of the central Alborz) is probably accounting for ~3 mm/yr (Nilforoushan et al., 2003; Vernant et al., 2004).

STRUCTURES

We divide the west-central Alborz into four structural zones that are roughly equivalent to the zones defined by Stocklin (1974a) (Fig. 2): (1) the northern zone (Stocklin's zone 3), where the intensity of deformation appears to increase southward from the northern foothills to the range crest. The southern boundary of the northern zone is the Kandavan thrust. (2) The thin-skinned zone (northern half of Stocklin's zone 4) is bounded by the Taleghan fault zone to the south and the Kandavan thrust to the north. This zone exhibits thin-skinned deformation largely limited to the Karaj Formation and overlying units. (3) The Taleghan range (within Stocklin's zone 4) is bounded by the Taleghan fault zone to the north and Mosha fault to the south. (4) The southern zone extends from the Mosha fault southward to the North Tehran and Farahzad-Karaj thrusts (Stocklin's zone 5). Deformation within this zone is by thin-skinned thrusting and is limited mainly to the Karaj Formation.

The Northern Zone

We studied faults in the intensely deformed region in the high Alborz, specifically the dextral Nusha fault, Barir fault zone, Tang-e-Galu fault zone, and the dextral-reverse Kandavan thrust (Figs. 2 and 4; Plates 1, 2, and 3). All of the northern- zone faults show dextral reverse kinematics along the main fault traces and sinistral normal kinematics on minor faults that intersect the larger faults. None of these faults shows any evidence of being active.

Dextral Nusha Fault

The Nusha fault (Fig. 4, stereonets 1 and 2) strikes northwest-southeast and is ~50 km long. The fault has two main splays. The Banan fault splays off the Nusha fault and extends westward, possibly as far as the westernmost Alborz (Figs. 2 and 4; Plate 1). The eastern Nusha fault splays into two strands, a northern strand that strikes roughly east-west and cuts a granitic intrusion of unknown age (Fig. 4; Plate 1) and a southern strand that strikes subparallel to the western Nusha fault and may intersect the northeastern edge of the Alam Kuh pluton (Figs. 2 and 4; Plate 1).

The Nusha fault offsets the Nusha pluton (98 ± 1 Ma; Lam, 2002) ~13 km dextrally. The main fault plane is subvertical, strikes ~120°, and has dextral Riedel shears, tension cracks, and tool marks. Striae and tool marks plunge <15° to the northwest and southeast (Fig. 4). At the outcrop scale, a second set of faults intersects the main dextral fault at high angles, with an average strike of ~180° and exhibits sinistral tension cracks, tool marks, and Riedel shears (Fig. 4).

Dextral Tang-e-Galu Fault Zone

The ~43-km-long Tang-e-Galu fault zone strikes northwest-southeast at the point where it is cut by the Alam Kuh pluton and curves eastward to an east-west strike. The fault zone splays eastward at a point ~7 km east of the Alam Kuh pluton (Figs. 2 and 4; Plates 1 and 3). Farther east, the Kojour thrust fault splays off the Tang-e-Galu fault (Fig. 2).

Between Dalir and Alam Kuh (Fig. 4, stereonets 3, 4, and 5; Plate 1), the main fault surface is subvertical, with an average strike of ~300° and exhibits dextral tension cracks, Riedel shears, and tool marks. Striations plunge <20° to the southeast and northwest (Fig. 4, stereonets 3, 4, and 5). At the outcrop scale, small northwest- to northeast-striking sinistral faults intersect the main dextral fault trace.

The Tang-e-Galu fault zone probably continues northwest of the Alam Kuh pluton and appears to cut and offset distinct assemblages of faults, folds, and strata by ~25 km. On its west side, northwest of the Alam Kuh pluton, this fault truncates a syncline-anticline pair (D and E on Fig. 4) and two subparallel fault strands (F and G on Fig. 4) that cut the south limb of the syncline and strike subparallel to the trend of this fold. Fault F juxtaposes Cretaceous volcanics interstratified with orbitolinid limestone to the north with the Jurassic Shemshak Formation to the south. Fault G lies to the south of fault F and juxtaposes the Jurassic Shemshak Formation to the north with Late Proterozoic rocks to the south (Fig. 4). On its east side, southeast of the Alam Kuh pluton, the fault zone cuts similar structures and strata (labeled on Fig. 4), suggesting that the folds and faults were once continuous prior to being cut and dextrally offset.

Dextral Barir Fault Zone

The ~20-km-long Barir fault zone strikes northwest-southeast and cuts the Akapol pluton, offsetting its margins by 3–5 km in a dextral sense (Figs. 2 and 4). The Barir fault zone merges with the Tang-e-Galu fault zone ~4 km southeast of the Akapol pluton and steps to the right near the western edge of the pluton (Figs. 2 and 4).

Kinematic indicators (tool marks, tension cracks, and Riedel shears) recorded along this fault zone show mainly dextral strike slip to oblique slip on a steeply northeast-dipping fault system that strikes ~330° (Fig. 4, stereonets 6 and 7). Striations and tool marks plunge between 80° and 10° to the northwest.

Dextral-Reverse Kandavan Thrust

The ~200-km-long Kandavan thrust is the southern boundary of the northern zone and thrusts Paleozoic rocks over Mesozoic and Cenozoic rocks along much of its length (Fig. 2; Plates 1, 2, and 3). This fault is pierced by the 6.8 ± 0.1 Ma Alam Kuh granite (Axen et al., 2001a). The granite, and granitic sills that can be traced back to the main granite body intrude the footwall and hanging wall of the Kandavan thrust and show no evidence of syntectonic intrusion or of deformation related to post–6.8 Ma reverse-dextral slip on the thrust.

The Kandavan thrust typically manifests as a zone of intense deformation, meters to tens of meters wide. Structural and kinematic data (Fig. 4, stereonets 8, 9, and 10) collected east of Alam Kuh indicate an average strike and dip for the thrust of ~290° and 35° to the northeast. Striations, Riedel shears, tension cracks, and tool marks indicate reverse dip slip and reverse-dextral oblique slip on most slip surfaces within fault-zone exposures (Fig. 4, stereonets 8, 9, and 10).

A dense network of high- and low-angle faults exists in the upper plate of the Kandavan thrust (Annells et al., 1975a, 1977; Vahdati Daneshmand, 1991; Guest, 2004). Figure 5A shows fault and slip-vector orientations for faults measured around map locations 1 and 2 on Figure 4. Most of these faults strike northwest-southeast and exhibit dextral, reverse, normal, and sinistral slip senses (Fig. 5A). In most cases, the relative ages of the different fault types could not be determined.

Figure 5B shows a photograph and stereonet for map location 3 on Figure 4. At this locality, northeast-dipping brittle fault planes form the margins of a 2-m-wide fault zone that thrusts Cambrian rocks over Ordovician rocks. Within the fault zone, tension fractures between two fault surfaces ~10 cm apart indicate normal and sinistral motion of the hanging wall (Fig. 5B), suggesting a reactivation of the thrust (?) that juxtaposed the Cambrian and Ordovician rocks.

The Thin-Skinned Zone

The thin-skinned zone tapers and switches structural vergence direction from west to east (Figs. 2 and 6; Plate 1; cross-sections A–A′ and B–B′ on Plate 2). In the Taleghan and Alamut region to the west, the zone is ~40 km wide,

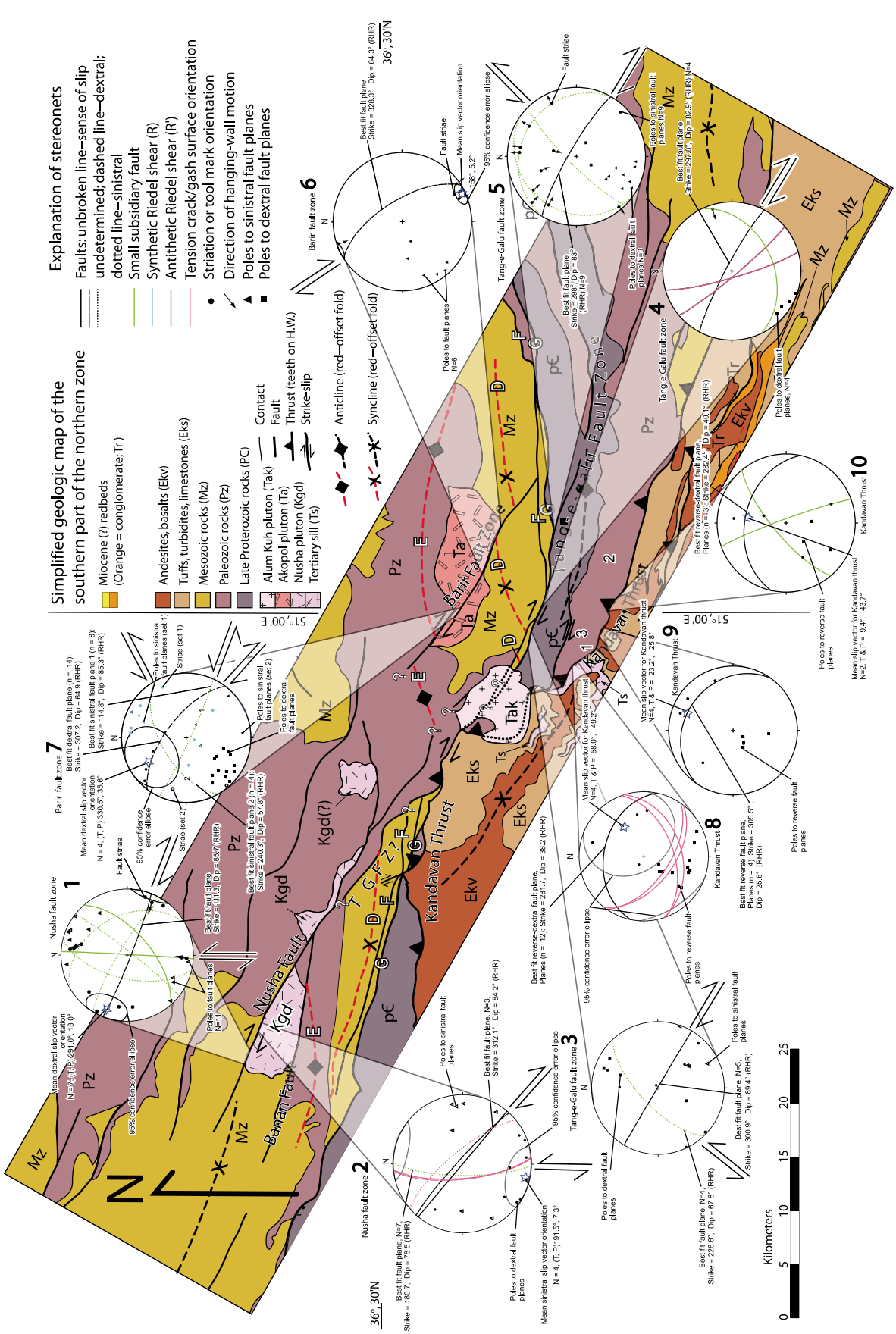

Figure 4. Map showing the portion of the northern zone that was examined in detail. Stereonet plots of structural data are tied to the locations where the data were collected. Letter and number labels indicate structures referred to in the text and in later figures.

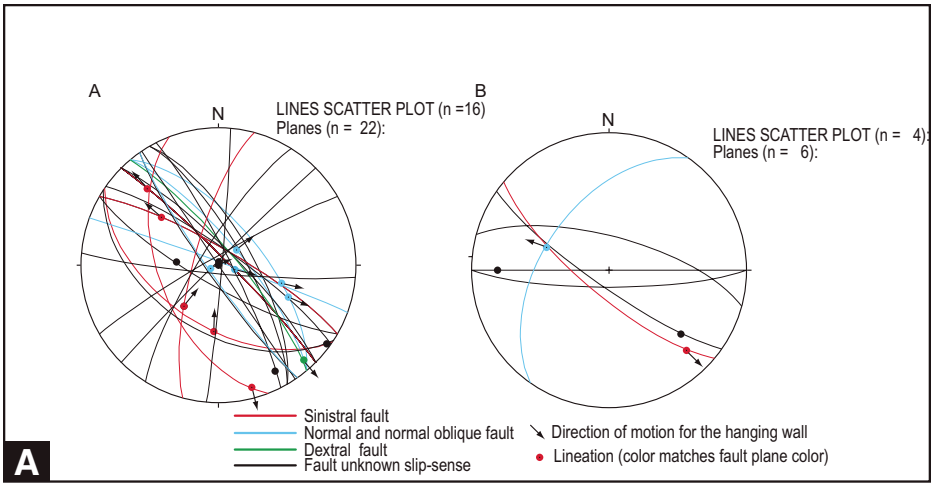

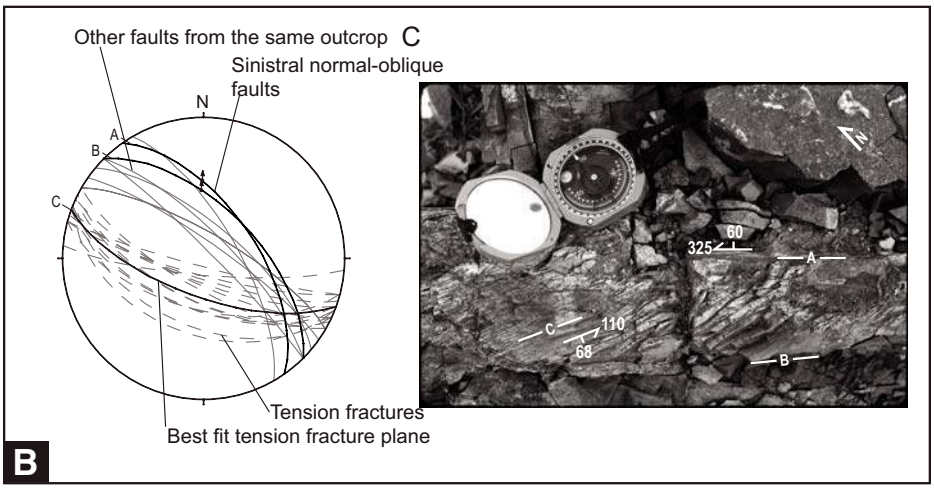

Figure 5. A: Two stereonet plots of faults measured at map locations 1 and 2 on Figure 4. B: Stereonet plot of faults and tension fractures measured in SW Dalir Valley, shown in photograph at right. Photograph was taken near map locality 3 (Fig. 4) looking downdip from outcrop containing two fault surfaces (A, B) bounding numerous tension fractures (gray dashed line). Compass is for scale, with compass needle indicating north. Fault planes dip NE (n = 8). Solid black lines are faults which bound tension fractures (A, B). Solid gray lines are faults in the same outcrop. Dashed gray lines are tension fracture planes (n = 14). Thick black line (C) represents cylindrical best fit of tension fracture planes. The faults juxtapose Cambrian Lalun Formation with Ordovician Lashkerak Formation; however, the arrows indicate a sinistral and normal sense of motion in the hanging wall.

exhibits broad open folds and steeply south-dipping faults (Figs. 2 and 6; Plate 1; cross-section B–B′ on Plate 2). To the east, the zone narrows to <10 km and exhibits tight to isoclinal folding and mainly north-dipping thrust faults that imbricate the Karaj Formation (Figs. 2 and 6; Plates 1 and 3; cross-section A–A′ on Plate 2).

There are five major thrusts within the eastern thin-skinned zone (Fig. 6; Plate 1). From north to south these are (informal names): the Piaz Chal thrust, upper Parachan thrust, lower Parachan thrust, Gar Ob thrust, and the Takieh thrust.

The Piaz Chal Thrust

The Piaz Chal thrust is located immediately south of the Kandavan thrust, from Upper Se Hezar Valley in the west to the eastern border of the study area (Fig. 6; Plate 1). The average dip of the Piaz Chal thrust is ~40° northeast, based on the outcrop trace of the fault (Fig. 6; Plates 1, 2, and 3). This fault emplaces upper-plate Karaj Formation tuffaceous clastic rocks over Karaj Formation andesite. The presence of shale and sandstone in the upper-plate hanging-wall flat suggests that this thrust soles into a décollement horizon within the Karaj Formation fine clastic sequence.

The Parachan Thrusts

The upper and lower Parachan thrusts (Fig. 6, stereonets 1 and 2; Plates 1, 2, and 3) extend from the eastern end of Alamut valley in the west to northeast of Gar Ob, where they merge with the Gar Ob thrust. These faults have best-fit fault-plane orientations (strike, dip, dip-direction) of 302°, 40° northeast for the upper Parachan thrust and 316°, 44° northeast for the lower thrust (Fig. 6, stereonets 1 and 2). Striations, tool marks, riedels, and tension cracks indicate near pure dip-slip, reverse motion on both faults.

The middle plate between the upper and lower Parachan thrusts is cut by steep faults (Fig. 6, stereonet 3; Plate 3). Most of these faults are oriented roughly orthogonal to the Parachan thrusts, exhibit dextral- and sinistral-oblique reverse and normal kinematics. Three of the middle-plate faults are oriented at ~45° to the main group of faults (Fig. 6, stereonet 3) and may represent conjugate faulting in the middle plate.

Stratigraphic separation across the upper Parachan thrust increases from <100 m in the eastern Alamut region to ~2 km in the Parachan area, and decreases eastward to <1 km (Figs. 2 and 6; Plates 1 and 3). In the Parachan area, the upper plate of this thrust is a hanging-wall flat composed of Karaj Formation tuff, shale, and sandstone.

Stratigraphic separation across the lower Parachan thrust increases from 0 km in the Alamut region to ~3 km north of Narijan, and then decreases eastward to <500 m east of Gar Ob, where the fault merges with the upper Parachan thrust (Plates 1 and 3). The upper plate of the lower Parachan thrust is a hanging-wall flat composed mainly of Karaj Formation andesite capped locally by minor amounts of Miocene red conglomerate. Slivers of Karaj Formation shale are locally exposed along the fault.

The presence of Karaj Formation andesite and clastic rocks in upper-plate hanging-wall flats of the lower and upper Parachan thrusts, respectively, suggests that these thrusts sole into décollement horizons within the Karaj Formation and do not cut older strata (Plates 1 and 2). That these faults merge to the southeast suggests that they merge at depth along strike to the northwest, and probably sole into the same décollement horizon.

The Gar Ob Thrust

The Gar Ob thrust system is exposed along the north side of the Taleghan River valley,

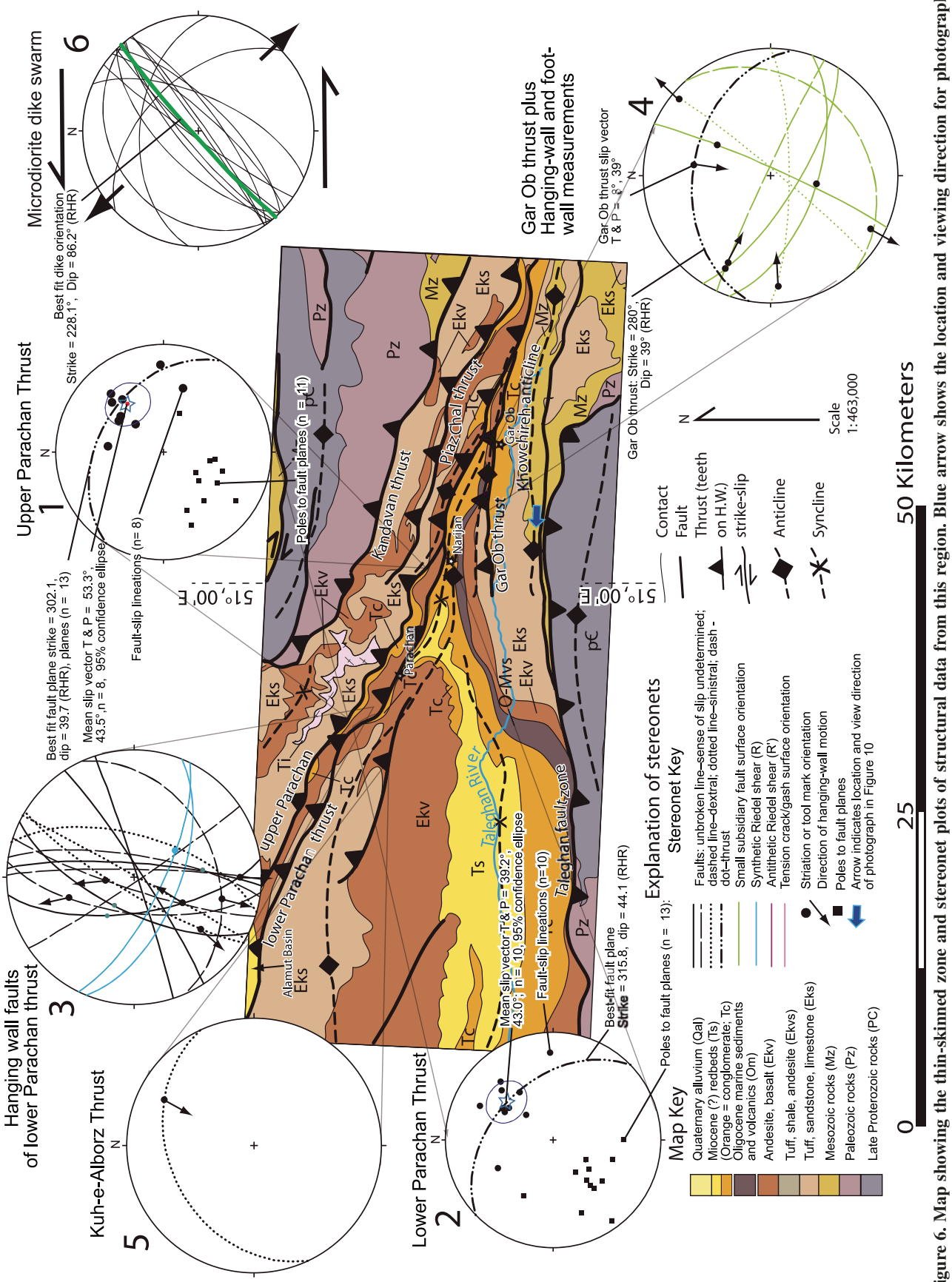

Figure 6. Map showing the thin-skinned zone and stereonet plots of structural data from this region. Blue arrow shows the location and viewing direction for photograph shown in Figure 7.

starting at a point ~15 km west of Gar Ob and continuing past Gar Ob to the east beyond the study area (Fig. 6, stereonet 4; Plates 1 and 3). It consists of several layer-parallel detachment horizons between 15 and 6 km west of Gar Ob, which merge and terminate in fault-cored fault-propagation folds (Plates 1, 2, and 3). The faults merge east of Gar Ob, where the fault is still nearly layer-parallel with a strike and dip of 280°, 39° northeast. Striations and mineral lineations on the fault surface indicate dip-slip, reverse motion (Fig. 6, stereonet 4). From ~5 km west of Gar Ob and beyond the town to the east, the Gar Ob thrust places upper-plate Karaj Formation rocks over Miocene conglomeratic growth strata deposited unconformably on the eroded north limb of the Khowchireh anticline (Fig. 6; Plates 1 and 3).

The Takieh Thrust

The Takieh thrust (Fig. 2; Plates 1 and 2) is a sinistral oblique thrust that crops out along the southwestern edge of Taleghan Basin and emplaces Karaj Formation lavas and clastics over conglomeratic growth strata of Taleghan Basin. This fault is well exposed near Takieh, but either terminates or is poorly exposed to the southeast. Maximum stratigraphic separation across this fault is ~3 km.

The Khowchireh Anticline

The Khowchireh anticline is ~5 km wide at its widest point and ~20 km long. Isoclinally folded Cretaceous Tiz Kuh limestone locally unconformably overlain by Paleocene Fajan conglomerate and Eocene Ziarat limestone is exposed in the core of the fold (Figs. 6 and 7; Plates 1, 2, and 3). These formations are cut by high- and low-angle normal faults that form horsts and grabens, over which tuffaceous mudstone and sandstone of the lower Karaj Formation clastic sequence was deposited (Fig. 7; Plates 1 and 3).

Dikes in the Thin-Skinned Zone

A microdiorite dike swarm intruded the thin-skinned zone during late Miocene time and in several localities cut the upper Parachan thrust. The dikes that cut the thrust were subsequently offset sinistrally along the thrust by ~20 m. Figure 6, stereonet 6 shows 14 microdiorite dike-margin measurements from the thin-skinned zone that have a best-fit strike and dip of 228°, 86° northwest. This orientation for the dike swarm is consistent with intrusion occurring in a sinistral shear kinematic regime with a tensile component oriented at 318°.

The Taleghan Range

The Taleghan range is a large, open, upright, gently west-plunging anticline with its limbs truncated by the high-angle Taleghan fault zone along its northern flank and by the Mosha thrust along its southern flank (Fig. 8; Plates 1, 2, and 3). Internally, the Taleghan range anticline is cut by numerous high-angle, normal- and reverse-separation faults of unknown age or slip sense (Annells et al., 1975a, 1977; Vahdati Daneshmand, 1991; Guest, 2004).

The Taleghan Fault Zone

The Taleghan fault zone is a sinistral-reverse fault that strikes east-west and extends along the northern margin of the Taleghan range (Fig. 8; Plates 1, 2, and 3). This fault zone typically consists of one to two fault gouge zones that are subvertical to south dipping and internally disorganized.

The western Taleghan fault zone typically consists of a single fault strand that juxtaposes Paleozoic and Mesozoic rocks to the south with Eocene Karaj Formation to the north. Fault gouge exposures along the western Taleghan fault zone exhibit dextral S-C fabrics and dextral-normal tension cracks, as well as sinistral-reverse S fabrics (Fig. 8, stereonets 1 and 2).

The eastern Taleghan Fault zone consists of two subparallel fault strands that bound slivers of tectonized Paleozoic and, more commonly, Mesozoic rocks, and juxtapose Paleozoic and Precambrian rocks to the south with Karaj Formation rocks and Miocene conglomerates of Taleghan Basin to the north (Fig. 8; Plates 1 and 3). Fault exposures along the eastern Taleghan fault zone exhibit sinistral-reverse tool marks, Riedel shears (R), and tension gashes (Fig. 8, stereonets 3 and 4).

The eastern Taleghan fault zone splits into northern and southern fault strands (Figs. 2 and 8; Plate 1). The northern strand strikes east-west and has Mesozoic rocks overlain by the Karaj Formation on both sides of the fault (Fig. 8, Plate 1). The southern fault strand bends southward and merges with the Mosha fault at the eastern terminus of the Taleghan range (Figs. 8 and 9).

The Mosha Fault

The Mosha fault dips north and strikes east-west in the west and northwest-southeast to the east. This fault extends for ~150 km within the southern Alborz, terminating beneath alluvium at the southern foot of the Taleghan range in the west and merging to the east with the Firuz Kuh fault in the east-central Alborz.

The western Mosha fault (Fig. 8; Plates 1 and 3) is a north-dipping sinistral-oblique thrust fault that juxtaposes Mesozoic, Paleozoic, and Precambrian rocks in the hanging wall with Eocene Karaj Formation rocks in the footwall. Fault exposures near the western terminus of the Mosha fault exhibit reverse dip– to sinistral-oblique-slip tension cracks, tool marks, and synthetic Riedel shears (R; Fig. 8, stereonet 5). To the east of the eastern terminus of the Taleghan range, exposures of the Mosha fault exhibit striations, tool marks, and tension cracks, indicating sinistral oblique-reverse slip (Fig. 8, stereonet 6). Small synthetic faults (Riedel shears [?]) in the hanging wall of the Mosha fault have reverse-dextral-oblique slip senses (Fig. 8, stereonet 6).

The Southern Folded Zone

The southern folded zone has a rhomboid shape in map view and is bounded by the Mosha fault to the north and the Farahzad-Karaj thrust and North Tehran thrust to the south (Fig. 8; Plate 1). This zone exhibits three sets of structures: (1) northwest-southeast–striking thrust faults, (2) a younger set of large, open to tight northwest-southeast–trending synclines and anticlines, which refold (3) an older set of folds that trend roughly northeast-southwest (Fig. 8; Plate 1).

All of the major thrusts in the southern folded zone appear to merge laterally (Figs. 2 and 8; Plate 1). The Farahzad-Karaj thrust merges with the North Tehran thrust to the east and Mosha fault to the west (Fig. 2), whereas the North Tehran thrust diverges from the Mosha fault ~20 km to the east of Tehran and rejoins the Mosha fault ~25 km northwest of Tehran (Figs. 2 and 8). The Purkan thrust merges with the Farahzad-Karaj thrust to the southeast and northwest (Fig. 8). The Dervaneh thrust (new name) merges with the North Tehran thrust immediately north of Tehran (Fig. 8). All of this suggests that the Farahzad-Karaj, Purkan, Dervaneh, and North Tehran thrusts merge with the Mosha fault at depth (Plate 2). This observation implies that the entire southern folded zone is a large transpressional duplex system.

The kinematics and geometries of the thrust faults in the southern folded zone are poorly constrained. The North Tehran thrust exhibits sinistral strike-slip and reverse-oblique striae, tension cracks, mineral fibers, and c fabrics in fault-plane exposures north of Tehran (Fig. 8, stereonet 7). The Purkan thrust cuts upsection to the west via four lateral ramps, the lower and upper edges of which are marked with red and yellow arrows, respectively, on Figure 8. The Dervaneh thrust fault is a splay off the North

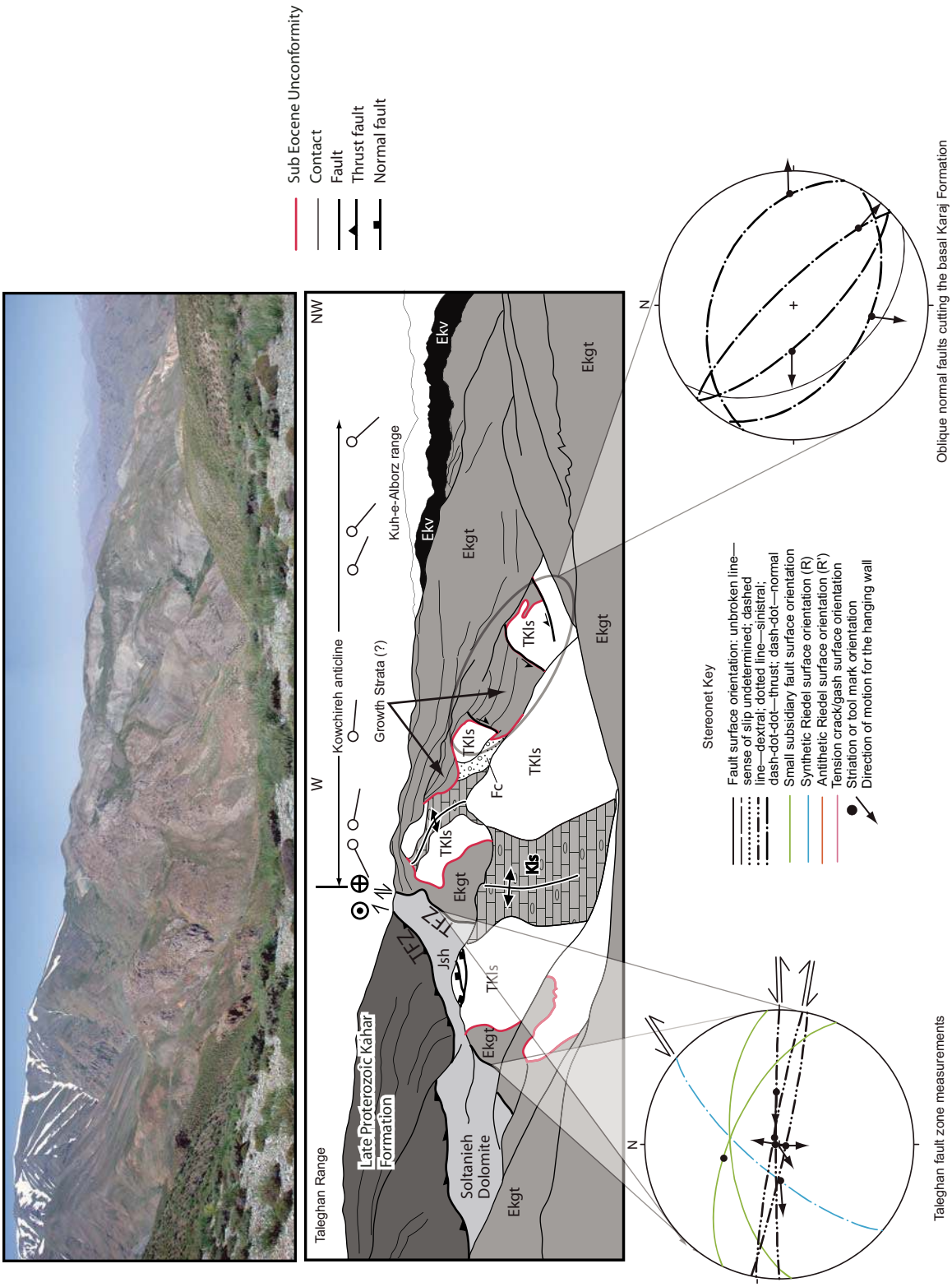

Figure 7. Photo with line drawing of Khowchireh anticline (blue arrow on Figure 6 shows location and viewing direction). Eocene tuffaceous clastic rocks (gray fill) are draped unconformably in Eocene normal fault–generated grabens. Faults cut Paleocene isoclinal folds in Cretaceous Tiz Kuh (Kls) limestone overlapped, locally, by Fajan conglomerate (Fc). To the south (left) Kahar Formation quartzites, Soltanieh dolomites (yellowish rocks), and carbonaceous Jurassic Shemshak Formation (Jsh, dark slope former) are juxtaposed with the younger units to the north across two strands of the sinistral-reverse Taleghan fault zone (TFZ; thrust and high-angle fault to north).

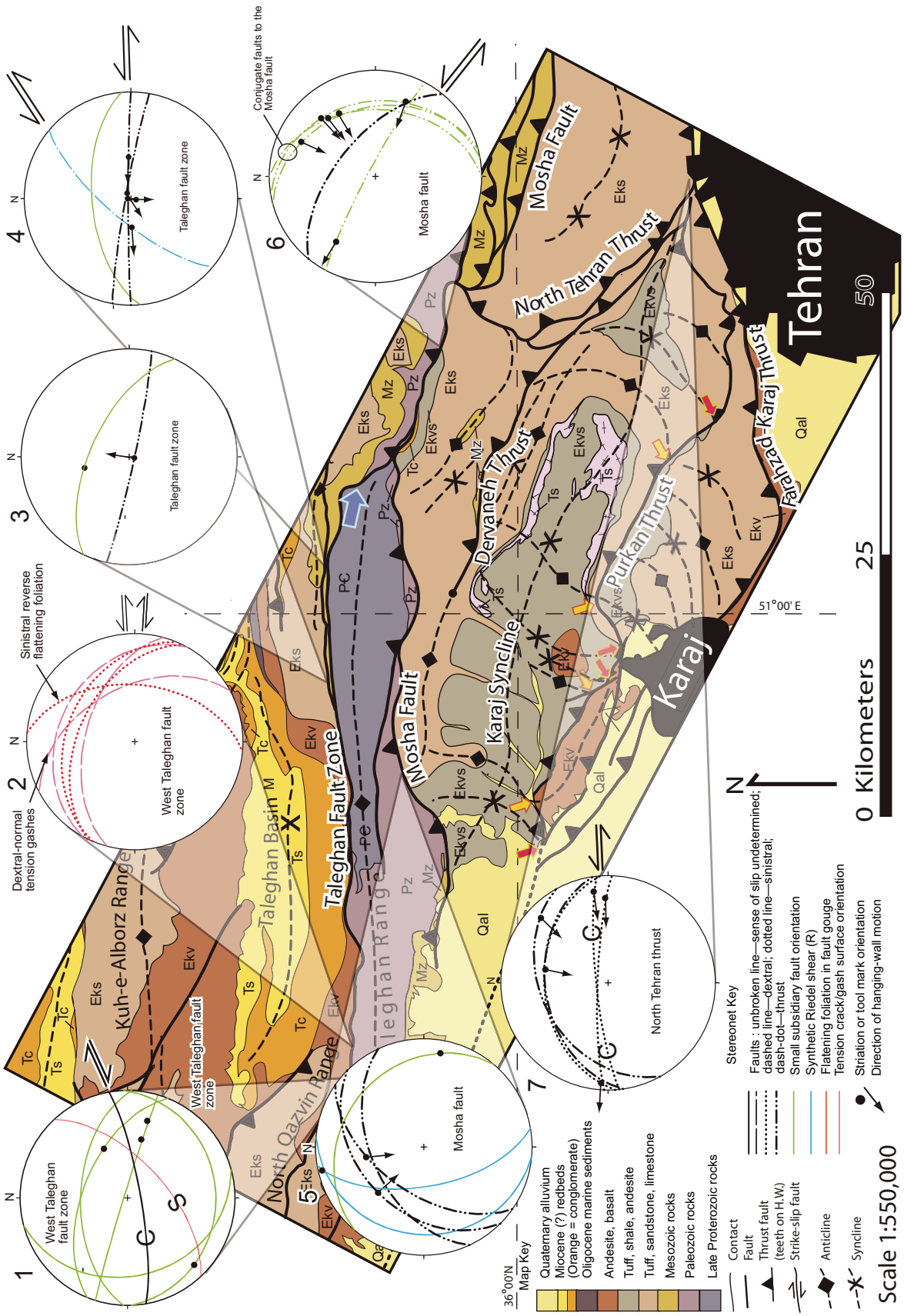

Figure 8. Map showing the Taleghan range and the southern folded zone and stereonet plots of structural data collected throughout this region. Blue arrow indicates the viewing direction and location of the region shown in Figure 9. Red and yellow arrows along the Purkan thrust show the locations of fault bends in this thrust that correspond to northeast-southwest–trending anticlines and synclines (fault-bend folds) in the upper plate. See Figures 4 and 6 for definitions.

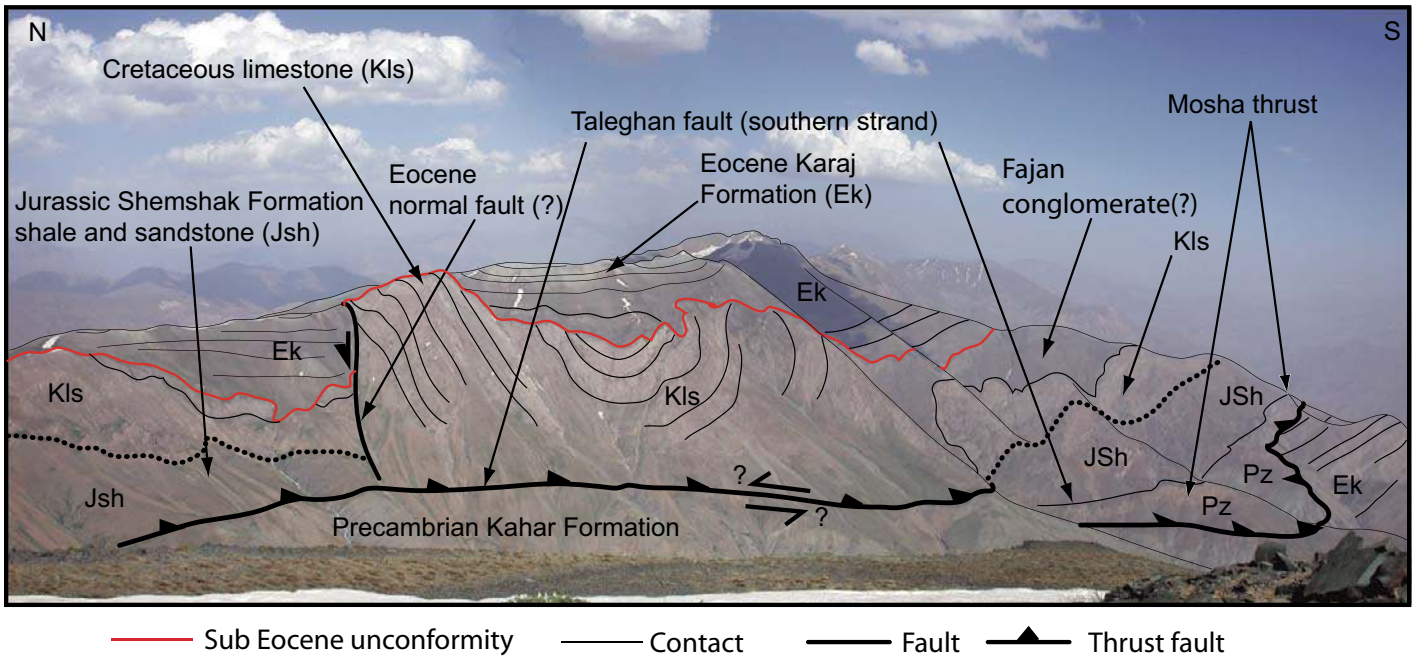

Figure 9. Photo with lines for clarity of the Mosha fault linking via a right bend to the Taleghan fault zone. The ridge line (hanging wall) exposes subhorizontal Eocene Karaj Formation (Ek) tuffaceous clastics deposited in an Eocene half graben over Paleocene-Eocene topography developed on folded Cretaceous limestones (Kls) (entire package in hanging wall of the Mosha-Taleghan fault zone). Footwall is Late Proterozoic Kahar Formation. North-tilted Karaj Formation tuffaceous clastics overlain by small amounts of Neogene conglomerate lie beneath the Mosha fault to the south. Jsh—Jurassic Shemshak Formation; Pz—Paleozoic rocks.

Tehran thrust and terminates to the west in the core of a fault-propagation anticline (Fig. 8; Plates 1 and 2).

We interpret the large open northwest-southeast–trending folds as hanging-wall synclines and anticlines that lie above frontal footwall ramps developed along the Purkan, Farahzad-Karaj, Dervaneh, and North Tehran thrusts. Tight northwest-southeast–trending folds are probably fault propagation folds (e.g., western tip of the Dervaneh thrust). The largest open fold (informally named the Karaj syncline) trends east-northeast–west-southwest and is exposed in the upper plate of the Purkan thrust. This syncline probably lies over a frontal footwall ramp in the Purkan thrust lower plate (Plate 1). Similar subparallel synclines lie in the upper plates of the Dervaneh and North Tehran thrusts.

Allen et al. (2003) suggested that the northeast-southwest–trending folds exposed in the thrust plate between the Dervaneh and Farahzad-Karaj thrusts may be related to an earlier, post-Eocene episode of local dextral transpression, where the compressional axis of the local strain ellipse was oriented northwest-southeast (orthogonal to the regional Miocene to Recent compressional axis). We cannot rule this interpretation out completely; however, we note that northeast-southwest–trending folds do not occur elsewhere in the central Alborz. We therefore prefer an interpretation that is consistent with their development in the present sinistral transpressional kinematic regime. One likely interpretation is that the small northeast-southwest–trending refolded folds are lateral-ramp anticlines and synclines (e.g., Dahlstrom, 1970; Boyer and Elliott, 1982). Those in the Purkan thrust plate are located above the lateral thrust ramps in the footwall of the Purkan thrust (Fig. 8; Plates 1 and 2), which suggests that they are geometrically related to the geometry of the Purkan footwall. The outcrop pattern of the Karaj syncline illustrates this (Fig. 8): the outcrop width of unit Ekvs in the syncline decreases dramatically from west to east across the western Purkan thrust footwall lateral ramp and then terminates west of the upper edge of the eastern Purkan thrust footwall lateral ramp, where the Ekvs is eroded away. Farther east, unit Ekvs reappears above the lower edge of the eastern Purkan footwall ramp. This suggests that the entire upper plate to the Purkan thrust, possibly including the Dervaneh thrust, is folded over the Purkan thrust footwall lateral ramps.

Northeast-southwest–trending refolded folds between the Purkan and Farahzad-Karaj thrusts do not appear to correlate with footwall ramps in the Farahzad-Karaj fault (Fig. 8). These folds could, however, have formed over small horses and/or duplex systems above the Farahzad-Karaj thrust. Detailed mapping is required in this region to better understand the mechanism driving this localized range-normal folding.

Cross Sections

Two cross sections (A–A′ and B–B′; Plate 2) incorporate the observations described herein. For these cross sections, we assume "kink-fold" fold geometries and base unit thicknesses on reported thicknesses in the literature (Sieber, 1970; Annells et al., 1975a, 1975b, 1977; Vahdati Daneshmand, 1991) and on thicknesses measured off Plate 1.

Section A–A′ extends through all zones to the Caspian coast and includes several strike-slip and oblique-slip fault zones. This structural style, combined with poor surface data and no subsurface data, generally results in nonunique structural interpretations. The cross sections presented on Plate 2 should therefore be considered as first-order interpretations of a limited data set. These structural interpretations do, however, allow us to make a reasonable estimate of fold-and-thrust–related range-perpendicular shortening using basic cross-section balancing techniques for the geology between

the strike-slip fault zones, and they give insight into the pre–late Cenozoic crustal architecture of northern Iran.

For section A–A′ on Plate 2, we restored deformation in the Karaj Formation and overlying units to the south of the Tang-e-Galu fault zone and the Cretaceous units to the north of the Tang-e-Galu fault zone. This restoration constrains post-Eocene shortening to the south and post-Cretaceous shortening to the north of the Tang-e-Galu fault zone (Plate 2).

The restoration of the Karaj Formation yields a minimum shortening estimate of 33.2 ± 1 km. The main problem with the restoration of the Karaj Formation is that in the thin-skinned zone (between the Kandavan thrust and the Taleghan fault zone), the shortening calculated for the imbricated upper plate of the décollement located just below the upper Karaj Formation volcanic section (Plate 2) is ~12 km greater than can be accounted for in the footwall of the décollement. The available data make it difficult to evaluate whether this discrepancy is related to tectonic thickening of the footwall rocks below the décollement by simple horizontal shortening, or to strike-slip removal of footwall material, or southward overthrusting of rocks north of the Kandavan thrust. Southward overthrusting is the most likely possibility and requires that the thin-skinned zone décollement extends to the north beyond the present position of the Kandavan thrust and carries in its hanging wall the entire upper-crustal stratigraphic section (Precambrian Kahar Formation and all overlying formations). This in turn implies that the décollement merges to the north with a north-dipping footwall ramp that cuts down through the entire upper-crustal stratigraphic section and merges with a deep basal décollement, which underlies the northern Alborz. To accommodate the entire upper-crustal stratigraphic section, to produce bedding orientations consistent with those observed to the north of the Kandavan thrust, and to account for the footwall shortening that is missing from beneath the thin-skinned zone, this footwall ramp would have to lie in the position presently occupied by the Tang-e-Galu fault zone (Plate 2). Finally, the position of this hypothetical footwall block beneath a region also dominated by strike-slip deformation suggests that this structure has been dismembered by subsequent or coeval strike-slip deformation. More geologic mapping is required to determine which of the aforementioned scenarios, if any, is true.

The available data for the regions around the Taleghan range suggest that a scenario such as this holds true in the southern Alborz. The restoration of the southern folded zone, Taleghan range, and the southern thin-skinned zone requires the presence of a major thrust ramp that would allow the Precambrian Kahar Formation to be carried up to the surface in its hanging wall (Plate 2). The position of the Khowchireh anticline and the magnitude of shortening required to generate the observed deformation in the southern folded zone are consistent with the presence of such a structure in the subsurface beneath the Taleghan range. The interpretation presented here (Plate 2) also requires that the southern ramp is cut and dismembered by strike-slip deformation.

Our restoration of Cretaceous and older units that lie to the north of the Tang-e-Galu fault zone yields ~2.8 km of range-normal shortening. Our interpretation of this area is strongly limited by the very sparse structural, kinematic, and stratigraphic data from this region. Based on the restoration of cross-section A–A′, we estimate total shortening across the Alborz to be 36 ± 2 km, which is in reasonable agreement with the estimate (~30 km) made by Allen et al. (2003). These estimates do not account for the movement of material into and out of the plane of cross section.

Section B–B′ is drawn through the western end of Taleghan Basin and the eastern end of Alamut basin from the Kandavan thrust in the north to the Taleghan fault zone in the south. Restoration of all layers yields ~12.5 km of shortening across this region. Most of the deformation postdates the formation of a large middle to late Miocene intramontane basin in this region (Guest et al., 2001; Guest, 2004). Extrapolation of this cross section to the range scale (Caspian to southern range margin) would yield only a little extra shortening, because the northern zone has so little shortening (e.g., ~3 km for A–A′), and the Taleghan range is narrow south of B–B′, where no equivalent of the southern folded zone exists. This shortening estimate of ~15–18 km (accounting for northern and southern contributions) is roughly half that presented by Allen et al. (2003) and determined for A–A′.

DISCUSSION

Alborz Shortening

Northern Zone

We conducted no more than a brief reconnaissance of the northern Alborz foothills; however, Stocklin (1974a), Huber and Eftekhar-nezhad (1978a, 1978b), Alavi (1996), and Allen et al. (2003) presented cross sections that include the northern zone. In their cross sections, Stocklin (1974a) and Huber and Eftekhar-nezhad (1978a, 1978b) showed several steeply south-dipping faults with ≤2 km of reverse slip along the north flank of the Alborz. These authors favored basement involvement for these structures as opposed to thin-skinned deformation, and Stocklin (1974a) suggested that the faults are inactive. Allen et al. (2003) noted the presence of seismicity along the north flank of the Alborz, and from this inferred basement involvement for the eastern segment of the Binaksar fault and the Kojour fault, which merges westward into the Tang-e-Galu fault zone. Allen et al. (2003) also inferred a possibly active blind thrust (Khazar fault) beneath the present Caspian coastline (Fig. 2). They speculated that this thrust is a basement-involved, south-dipping structure with north-dipping back thrusts that break the surface along the northern foothills of the Alborz (Fig. 2).

Although there are small-displacement faults located along the northern foothills of the Alborz, their slip sense, length, and throw remain poorly constrained or undetermined. Furthermore, active surface breaks predicted by the accumulation of slip on the Khazar thrust ramp and active back-thrust development, respectively, are not mapped along the north edge of the range. It is therefore difficult, even with the evidence for seismicity, to confirm the presence of the Khazar fault or some other major, long-lived, north-vergent, active blind thrust along the north edge of the west-central Alborz. More basic structural and seismic studies of the northern margin of the Alborz are needed, so that the spatial distribution of active deformation across the range can be better constrained.

Following Stocklin (1974a), we suggest that the northern zone faults are smaller and less active than those to the south. The Tang-e-Galu fault zone, Barir fault zone, and Nusha fault zone all exhibit dominantly dextral kinematics. In each of these cases, subsidiary sinistral faults intersect the main dextral fault traces at high angles (>75°) and are probably conjugate faults that formed in the now-inactive local dextral kinematic regime (Fig. 10). Only the hanging wall of the dominantly dextral-reverse Kandavan thrust shows any evidence of reactivation of previously dextral faults in the presently active, regional sinistral kinematic regime (Fig. 5).

In our restored cross section (Plate 2), the region north of the Tang-e-Galu fault zone (Fig. 2; Plates 1 and 2) exhibits 2.8 km of shortening (less than 10% of the total shortening estimated across the range). This and the minimal drop in GPS velocity across the northern Alborz (~1 mm/yr between sites MEHR and MAHM; Vernant et al., 2004) support the suggestion that the northern zone did not accumulate much internal shortening in the past and is not accommodating much internal shortening at the present time.

In contrast, the northern zone appears to have accommodated a significant amount of strike-slip deformation. The Nusha and Barir

faults accumulated 12 km and 2–4 km of dextral strike-slip motion, respectively. Dextral strike-slip motion on the Tang-e-Galu fault is estimated to be ~25 km (Figs. 6 and 10). The amount of dextral strike-slip motion accommodated by the Kandavan thrust and the Banan fault is unknown. Detailed mapping in this region is limited; for example, if we assume that the Nusha, Tang-e-Galu, and Barir faults are linked and feed slip into one another, then we tentatively estimate at least 25–30 km of cumulative dextral shear across the southern margin of the northern zone (Fig. 10). If, on the other hand, the Nusha and Tang-e-Galu faults are not linked, cumulative dextral shear is probably greater and in the range of 38–41 km.

The timing of this dextral deformation is uncertain. The dextral-reverse Kandavan thrust clearly cuts middle Miocene gravels (Guest, 2004), which suggests that this fault was active during or after middle Miocene time. It is possible, therefore, that the dextral strike-slip faults to the north of the Kandavan thrust were active at this time as well. Activity on some of these structures clearly ceased prior to 6.8 ± 0.1 Ma, when the Alam Kuh pluton pierced the Kandavan and Tang-e-Galu fault systems and possibly the southeastern extension of the Nusha-Banan fault system (Fig. 4). It is unclear, however, whether the Barir fault and other dextral faults not cut by Alam Kuh pluton were active after ca. 6.8 Ma.

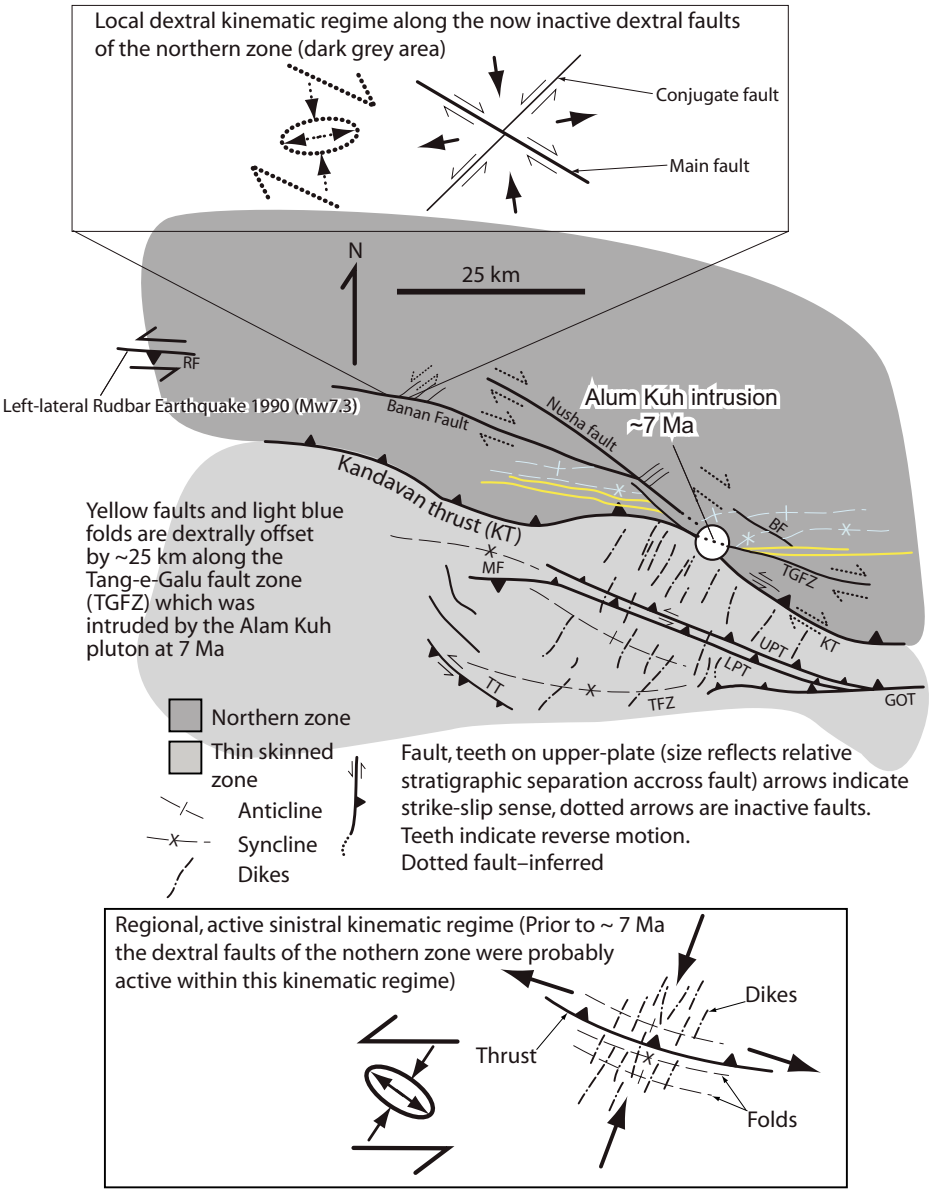

Figure 10. Schematic fault map of the northern zone and thin-skinned belt showing the kinematic regimes that control the orientation and kinematics of the small and large structures in the region (see Figure 4 for an explanation of abbreviations). In the northern zone (dark-gray area), small sinistral conjugate faults intersect the major dextral faults at the outcrop scale. Offset markers (yellow faults and light-blue folds) for the Tang-e-Galu fault zone (TGFZ) indicate ~25 km of dextral offset. In the thin-skinned belt, a microdiorite dike swarm intruded at ca. 6–9 Ma. The dikes are roughly orthogonal to thrusts and folds and locally intruded across, and were subsequently offset by, thrust faults (e.g., upper Parachan thrust [UPT]). This suggests that the dikes intruded parallel to the shortening direction during active contractional deformation.

Thin-Skinned Zone

The thin-skinned zone shows strong evidence of late Miocene deformation. The thrust faults of the thin-skinned zone generally strike northwest-southeast, whereas the late Miocene microdiorite dike swarm that intrudes the thin-skinned zone cuts across but is slightly offset by the thrusts, and strikes northeast-southwest (Fig. 6; Plate 3). The dike swarm probably intruded parallel to the maximum compression direction, and the thrust faults developed perpendicular to the maximum compression direction. The orientations of the thrusts and the dike swarm and their synchronous development suggest that the thin-skinned zone was active during and possibly after late Miocene time and that it evolved in a sinistral-shear kinematic regime (Fig. 10).

Taleghan Range

The Taleghan range shows evidence of long-term activity. The Taleghan fault zone is broad, composed of multiple fault strands, and it exhibits dextral-normal and sinistral-reverse kinematics, suggesting that the fault zone was a dextral-normal fault zone that was subsequently reactivated as a sinistral-reverse system. Reactivation of the Taleghan fault zone is supported by map patterns indicating that the southern strand of the eastern Taleghan fault, just north of where it merges with the Mosha fault, is a sinistral-oblique thrust fault that thrusts Paleozoic rocks over Precambrian rocks (Fig. 8; Plate 1). This requires that the southeastern strand of the Taleghan fault was previously a normal fault that dropped Paleozoic rocks down to the northeast against the Precambrian rocks in its footwall. Now reactivated as a reverse-oblique thrust, the fault carries the formerly down-dropped hanging wall back up over its Precambrian footwall.

If the Taleghan fault zone was a dextral normal fault that dropped the north and northeast side down, then this suggests that the Taleghan range was elevated relative to the region to the north and possibly the south. This is supported by thinning of the Karaj Formation by >1 km across the Taleghan range (Plate 2) and the presence of normal faults in the basal Karaj Formation clastic sequence, which provided accommodation space for the Karaj Formation sediments (Figs. 7 and 8).

The Mosha fault shows no evidence of reactivation and continues as a sinistral-oblique thrust beyond the eastern edge of the study area. Northeast of Tehran, the Mosha fault bends to the north and changes to a left-lateral strike-slip fault, which is argued to have accumulated ~30–35 km of left-lateral displacement (Allen et al., 2003). Ritz et al. (2003) tentatively estimated a slip rate of 2.7 ± 0.5 mm/yr for this fault, based on preliminary geomorphic investigations in the region northeast of Tehran. For 30–35 km of slip to accumulate at a constant slip rate of 2.7 ± 0.5 mm/yr requires 12.6 ± 3.2 m.y., which is in good agreement with the ca. 12 Ma estimate for the onset of late Cenozoic deformation in the Alborz (Guest, 2004) and suggests that the Mosha fault has been active since that time.

If the Mosha fault has accumulated ~30–35 km of sinistral slip 50 km east of Tehran, then we should be able to account for this amount of slip to the west of Tehran. Here we suggest that the Mosha fault merges with the Taleghan fault zone via the southwestern Taleghan fault strand (Figs. 8 and 9; Plate 1). If the Mosha fault transfers left-lateral slip to the Taleghan fault zone, then the Taleghan and Mosha fault systems can be viewed as a single sinistral strike-slip system that has a major right-hand bend (Fig. 11).

The along-strike kinematics and geometry of the Mosha fault are consistent with this view. Figure 8, stereonets 5 and 6, indicate that the Mosha fault changes from a strike-slip fault northwest of Tehran to a thrust fault farther west. Furthermore, stratigraphic separation across the western Mosha fault decreases to the west, which probably reflects a westward decrease in total slip on the fault (Fig. 8; Plate 1). We therefore suggest that a portion of the slip on the eastern Mosha fault is transferred to the Taleghan fault zone. The amount of slip transferred, however, is unclear and requires a more detailed investigation of the Mosha and Taleghan fault zones, especially the southeastern Taleghan fault strand.

Southern Folded Zone

The southern folded zone is a duplex system that probably developed in response to transpression across the right-hand bend in the Mosha-Taleghan fault system, analogous to the way the left-hand bend in the dextral San Andreas fault has induced transpressional thrusting and folding in southern California. Similar to southern California, the thrust faults and folds in the southern folded zone are oriented subparallel to the bent segment of the Mosha thrust (Fig. 11). The sinistral strike-slip and reverse oblique-slip kinematic indicators observed on the North Tehran thrust near Tehran are consistent with this fault and, farther west, the east-west–striking segment of the Farahzad-Karaj fault, being a tear fault system that accommodates the development of the southwest-vergent duplex system to the north.

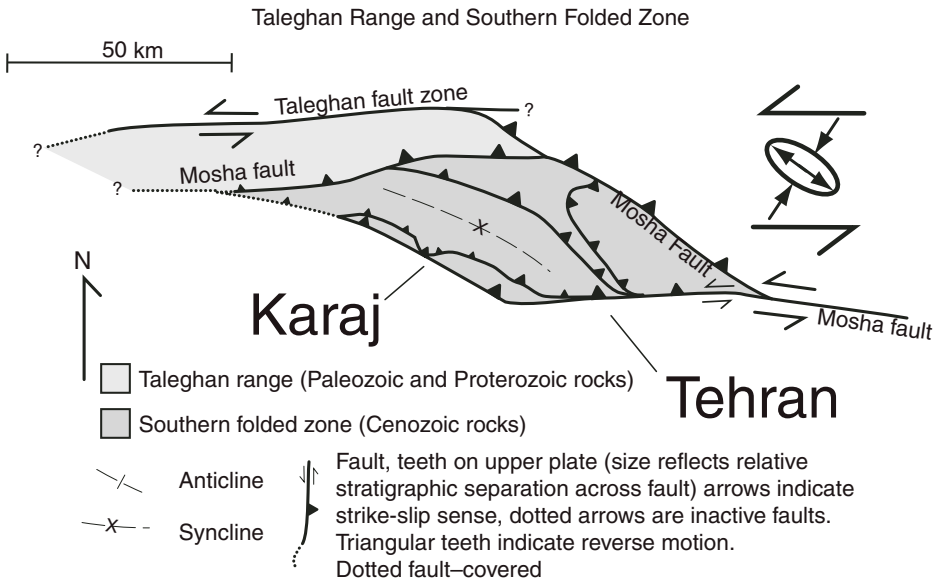

Figure 11. Schematic fault map of the Taleghan range and southern folded zone showing the right-hand bend in the Mosha-Taleghan fault system and adjacent transpressional deformation.

Strain-Rate Comparisons

The ~30 km (Allen et al., 2003) and 36 ± 2 km (this paper) shortening estimates for the Alborz are generally inconsistent with the 5 ± 2 mm/yr shortening rate across the range based on GPS surveys and the ca. 12 Ma estimate for the onset of deformation in the Alborz (Guest, 2004). A constant shortening rate of 5 ± 2 mm/yr over ~12 m.y. yields a net shortening of ~60 ± 24 km across the Alborz. One possible solution to this apparent inconsistency incorporates strike-slip deformation in the shortening estimate across the range (Fig. 12). This model assumes that, prior to ca. 5 Ma, the dextral strike-slip faults of the northern zone (Nusha, Banan, Barir, Tange-Galu, and Kandavan faults) were active and formed part of a conjugate strike-slip system with the sinistral Taleghan-Mosha fault system (Fig. 12). The fault-bounded wedge caught between the northern dextral and southern sinistral fault systems moved ~20 km to the west along the Mosha-Taleghan fault system between ca. 12 Ma and ca. 5 Ma, based on the Vernant et al. (2004) 2.7 ± 0.5 mm/yr slip-rate estimate (Fig. 12). This predicts ~27 km of dextral slip on the northern fault system, which is consistent with the tentative 25–30 km maximum dextral displacement estimated for this region. This model also predicts ~17 km of strike-slip–related range-perpendicular shortening, which when added to the shortening estimates from restored cross sections (~36 km to ~30 km; this paper; Allen et al., 2003) yields ~47–53 km of shortening across the Alborz, well within error of the ~60 ± 24 km shortening estimate based on a constant 5 ± 2 mm/yr shortening rate since ca. 12 Ma. Furthermore, this model is kinematically feasible in a regime of regional sinistral shear and suggests that the Alborz could have developed in a state of sinistral transpression since middle Miocene time, without the need for a kinematic reversal from dextral to sinistral strike slip.

Shortening within the tectonic wedge coeval with its relative motion to the west predicts that the orientation of the boundary shear zones changed with time (Fig. 12). Cross-section B–B′ indicates ~12.5 km of shortening within the tectonic wedge, and the ca. 6–9 Ma dikes (Guest, 2004) that cut the faults and folds of the thin-skinned belt (also within the wedge) indicate that shortening of this region was

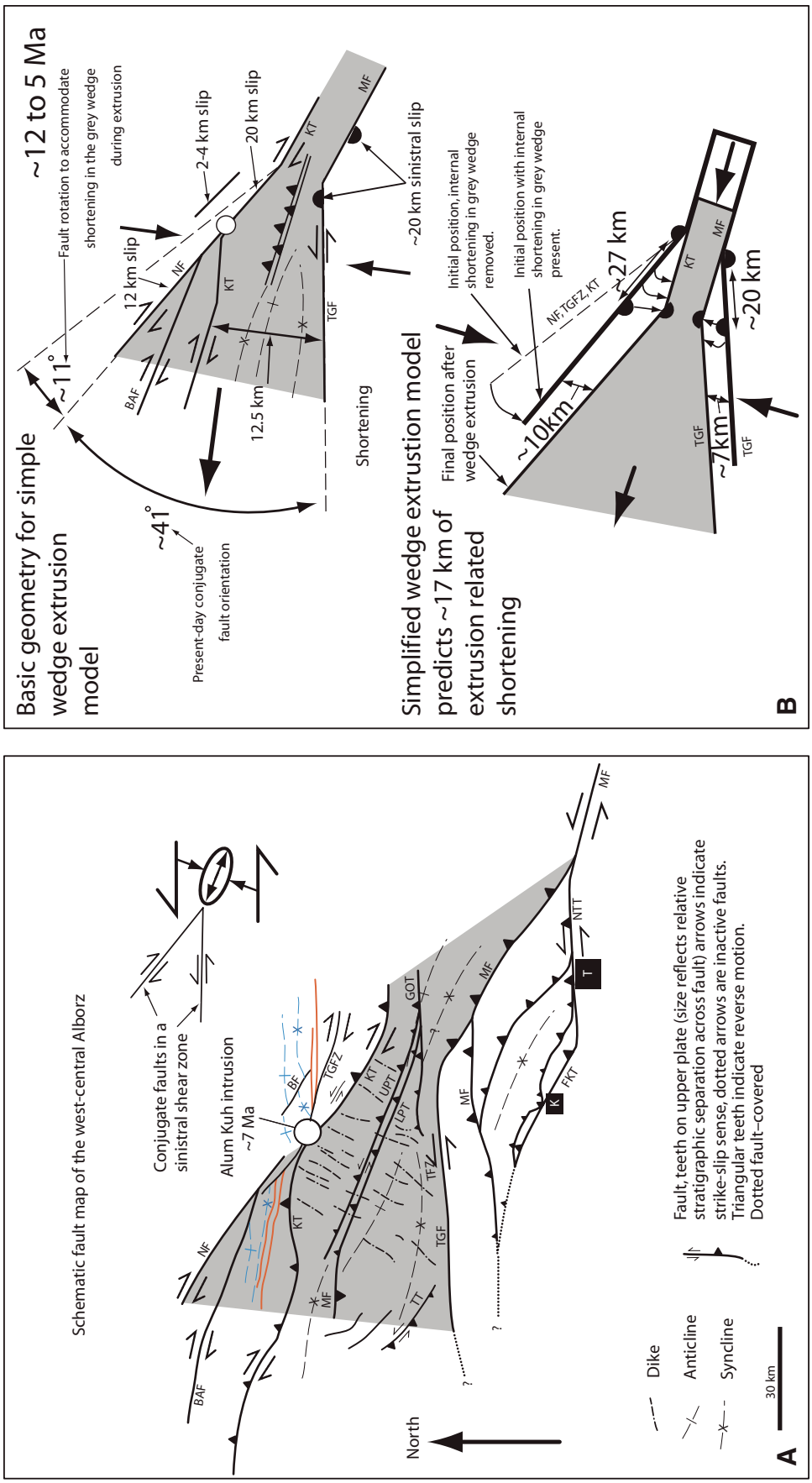

Figure 12. A: Schematic fault map of the west-central Alborz showing the presence of a tectonic wedge (gray shaded region) bounded by the dextral Nusha, Banan, Tang-e-Galu, and Kandavan faults to the north and the Mosha-Taleghan fault system to the south. This is probably a conjugate fault system that developed in a sinistral-transpression kinematic regime. B: Geometric representations of this conjugate system. Top shows the angle between the conjugate faults before 12.5 km of internal shortening within the wedge accumulates (~52°) and the present angle (41°). The 30 km estimated slip in the Mosha thrust is represented by offset, black half circles. Bottom shows a simplified geometric wedge extrusion model that predicts ~17 km of range-perpendicular strike-slip shortening when the wedge is extruded to the west, such that ~20 km of sinistral slip accumulates on the Mosha-Taleghan fault system and ~27 km of slip accumulates on the dextral system to the north.

occurring prior to and at least for a short time after ca. 6 Ma. The average angle between the present Mosha-Taleghan fault system and the Nusha–Tang-e-Galu system is ~41° (Fig. 12), similar to the ~48° angle between the conjugate San Andreas and Garlock faults and the ~42° angle between the conjugate Awong Co and Bue Co faults in western Tibet (Taylor et al., 2003).

Restoring the 12.5 km of shortening within the tectonic wedge rotates the wedge boundary faults apart by a combined ~11°, bringing the initial angle between the northern and southern conjugate fault systems to ~52°. This is a reasonable initial conjugate fault angle, considering that such systems have developed with similar angles all over the world (Turkey, southern California, and Tibet). However, it is inconsistent with the 120° angle expected from simple Andersonian fault theory (Anderson, 1951).

The cessation of dextral strike-slip deformation in the northern zone during latest Miocene time (ca. 5 Ma), based on the timing of dike intrusions and thrusting into the thin-skinned zone (tectonic wedge), probably marks a shift from shortening partitioned into conjugate strike-slip wedge motion and range-normal folding and thrusting to the present mode of deformation, which seems to be dominated by sinistral transpressional deformation focused along the south flank of the range and does not include a significant dextral component. Local compressional features, like the southern folded zone (this paper), and local extensional features, like those exposed along some segments of the Mosha-Taleghan fault system (Ritz et al., 2003), likely reflect complexity along the strike-slip fault systems rather than regional range-scale shortening or extension.

All of the observations presented so far and our tentative kinematic model have implications for our understanding of how strain accumulation over the long term (millions of years) compares with instantaneous strain measurements. We have shown evidence for a strong along-strike finite-shortening gradient in west-central Alborz, from ~53 km at cross-section line A–A′, ~40 km west of the Vernant et al., (2004) campaign GPS transect, to <20 km at cross-section B–B′, ~40 km farther west. Assuming that deformation along the Alborz began at ca. 12 Ma, this implies an along-strike gradient in shortening rate within the west-central Alborz ranging from ~5 mm/yr at cross-section A–A′ to ~1.5 mm/yr at cross-section B–B′. If accurate, this result suggests that transpressional mountain belts with complex long-term strain histories are likely to yield local long-term strain rates that are in disagreement with instantaneous strain rates derived from regional GPS surveys or from single across-strike transects. Future GPS surveys of complex transpressional belts should therefore include several across-strike campaigns that will allow for the detection of along-strike velocity gradients within the orogenic belt being studied.

Alborz Structural Models

Based on our observations and interpretations, we can evaluate the structural models of the Alborz presented by Stocklin (1974a), Şengör (1990), Alavi (1996), and Allen et al. (2003).

The thin-skinned, antiformal stack and orogenic collapse model presented by Alavi (1996) for the entire Alborz is, in general, inconsistent with our observations. Thin-skinned deformation in the western Alborz is present in the thin-skinned belt and southern folded zone but is generally limited to these regions and does not serve to build a range-scale antiformal stack (see cross-section A–A′, Plate 1).

Normal faults observed in the western Alborz belong to three groups. Eocene normal faults are overlapped by Karaj Formation sediments and were probably part of the extensional episode that accommodated the formation of the Karaj Formation sedimentary basin. Normal faults in the thin-skinned belt are orthogonal to the thrust faults and parallel to the late Miocene microdiorite dike swarm. These normal faults probably formed as tension shears as deformation in the thin-skinned belt progressed. Active extensional features along the Mosha-Taleghan fault zone (Ritz et al., 2003) are probably related to local releasing bends in this generally anastomosing left-lateral fault zone. Faults with normal separations in the northern zone may be older normal faults related to Eocene extension, or they may be strike-slip faults that merely have normal separations. More work on faults in the northern zone is needed before we can fully evaluate the significance of normal faulting in the northern Alborz.

The symmetrical transpressional flower structure model presented by Allen et al. (2003) is partially consistent with our observations. We observe that transpressional deformation along the south side of the Alborz appears to accommodate most of the transpression across the western Alborz. Our observations, combined with GPS velocities (Vernant et al., 2004), suggest that active deformation along the north side of the west-central Alborz does not appear to accommodate a large amount of convergence in northern Iran. The cross-sectional geometry of the Alborz is probably that of a southward-leaning asymmetrical flower structure that exhibits minor thrusting along its northern flank (e.g., Şengör, 1990).

CONCLUSIONS

1. Sinistral transpressional upper-crustal shear across the western Alborz appears to have been partitioned into strike-slip faulting and thin-skinned thrusting and folding since late Miocene time and has resulted in variable shortening amounts across the belt, ranging locally from ~53 ± 2 km of shortening in the eastern portion of the study area to as little as 15–18 km of shortening in the western portion of the study area.

2. The eastern shortening estimate (53 ± 2 km) was determined for a cross-section line that lies ~40 km to the west of the GPS transect of Vernant et al. (2004) and is within error of the 5 ± 2 mm/yr GPS-derived shortening rate across the Alborz (Vernant et al., 2004), and the ca. 12 Ma estimate for the onset of deformation in the Alborz (Guest, 2004), which predicts ~60 ± 24 km of shortening for a constant shortening rate since ca. 12 Ma.

3. The western shortening estimate (15–18 km) was determined for a cross-section line that lies ~80 km to the west of the GPS transect and suggests a much lower shortening rate (1.25–1.5 mm/yr) since ca. 12 Ma (assuming a constant shortening rate). This suggests that we need GPS control along transpressional mountain belts as well as across them before we can compare the instantaneous and long-term strain fields.

4. Between ca. 12 Ma and ca. 5 Ma, transpressional shortening in the Alborz was accommodated by generally southwest-vergent, thick- and thin-skinned thrusting and folding, and conjugate dextral and sinistral strike-slip faulting. Post–5 Ma, near-surface deformation has been limited to sinistral faulting and thrusting concentrated along the south flank of the range, though lack of data, high-precipitation rates, and vegetation along the north side of the range may obscure active structures in this region. Deactivation of the dextral fault system may be due to internal shortening and rotation of the dextral fault systems out of the optimum orientation for conjugate slip. Alternatively, this could be due to a change in the regional stress field between northern Iran and the south Caspian at ca. 5 Ma.

5. In the vicinity of Tehran, the Mosha fault and Farahzad-Karaj and North Tehran thrusts delineate a large transpressional duplex system that is developing adjacent to the right-hand bend in the Mosha-Taleghan sinistral fault system. This system is analogous to transpressional deformation in Southern California that is related to the left-hand bend in the San Andreas fault. Further study of this system should be carried out for seismic risk assessment in the heavily populated Tehran and Karaj urban areas.

ACKNOWLEDGMENTS

This research was supported by the National Science Foundation (grant EAR-9902932 to G.J. Axen), University of California–Los Angeles (UCLA) Council on Research (G.J. Axen), the University of Tehran Research Council (grant 651/1/328 to J. Hassanzadeh), and a UCLA Department of Earth and Space Sciences Cross-Training Fellowship (B. Guest and G. Peltzer). G. Peltzer provided critical advice and assistance with the remote sensing component of the mapping presented here. Early drafts of this manuscript were improved greatly by informal reviews from Nathan Niemi and Charlie Verdel. The insightful reviews returned by Nadine McQuarrie and Mark Allen led to significant improvements in the plates and in the text. Kevin Mahan reviewed a final version of the manuscript before final submission.

REFERENCES CITED

Alavi, M., 1996, Tectonostratigraphic synthesis and structural style of the Alborz mountain system in northern Iran: Journal of Geodynamics, v. 21, no. 1, p. 1–33, doi: 10.1016/0264-3707(95)00009-7.

Allen, M., Ghassemi, M.R., Shahrabi, M., and Qorashi, M., 2003, Accommodation of late Cenozoic oblique shortening in the Alborz range, northern Iran: Journal of Structural Geology, v. 25, no. 5, p. 659–672, doi: 10.1016/S0191-8141(02)00064-0.

Anderson, E.M., 1951, The dynamics of faulting and dyke formation with applications to Britain: Edinburgh, Oliver and Boyd, 206 p.

Annells, R.N., Arthurton, R.S., Bazley, R.A., and Davies, R.G., 1975a, Explanatory text of the Qazvin and Rasht quadrangles map: Tehran, Geological Survey of Iran, 94 p.

Annells, R.N., Arthurton, R.S., Bazley, R.A., and Davies, R.G., 1975b, Geological quadrangle map of Iran, Qazvin and Rasht sheet: Tehran, Geological Survey of Iran, scale 1:250,000.

Annells, R.S., Arthurton, R.S., Bazley, R.A.B., Davies, R.G., Hamedi, M.A.R., and Rahimzadeh, F., 1977, Geological map of Iran, Shakran sheet 6162: Tehran, Geological Survey of Iran, scale 1:100,000.

Assereto, R., 1966, The Jurassic Shemshak Formation in central Elburz (Iran): Reviews in Italian Paleontology and Stratigraphy, v. 72, no. 4, p. 1133–1182.

Axen, G.J., Lam, P.J., Grove, M., Stockli, D.F., and Hassanzadeh, J., 2001a, Exhumation of the west-central Alborz Mountains, Iran, Caspian subsidence, and collision-related tectonics: Geology, v. 29, no. 6, p. 559–562, doi: 10.1130/0091-7613(2001)029<0559:EOTWCA>2.0.CO;2.

Axen, G.J., Stockli, D.F., Lam, P., Guest, B., and Hassanzadeh, J., 2001b, Implications of preliminary (U-Th/He cooling ages from the central Alborz Mountains, Iran: Geological Society of America, Abstracts with Programs, v. 33, no. 7, p. 257

Berberian, F., and Berberian, M., 1981, Tectono-plutonic episodes in Iran, *in* Gupta, H.K., and Delany, F.M., eds., Zagros–Hindu Kush–Himalaya geodynamic evolution: Geodynamics Series: Washington, D.C., American Geophysical Union, p. 5–32.

Berberian, M., 1983, The southern Caspian: A compressional depression floored by a trapped, modified oceanic crust: Canadian Journal of Earth Sciences, v. 20, p. 163–183.

Berberian, M., and King, G.C.P., 1981, Towards a paleogeography and tectonic evolution of Iran: Canadian Journal of Earth Sciences, v. 18, p. 210–265.

Boyer, S.E., and Elliott, D., 1982, Thrust systems: The American Association of Petroleum Geologists Bulletin, v. 66, no. 9, p. 1196–1230.

Dahlstrom, C.D.A., 1970, Structural geology in the eastern margin of the Canadian Rocky Mountains: Bulletin of Canadian Petroleum Geology, v. 18, no. 3, p. 332–406.

Dehghani, G.A., and Makris, J., 1984, The gravity field and crustal structure of Iran: Neues Jahrbuch für Geologie und Palaontologie Abhandlungen, v. 168, no. 2/3, p. 215–229.

Dewey, J.F., and Şengör, A.M.C., 1979, Aegean and surrounding regions: Complex multiplate and continuum tectonics in a convergent zone: Geological Society of America Bulletin, v. 90, p. 84–92, doi: 10.1130/0016-7606(1979)90<84:AASRCM>2.0.CO;2.

Guest, B., 2004, The thermal, sedimentological and structural evolution of the central Alborz mountains of northern Iran: Implications for the Arabia-Eurasia continent-continent collision and collisional processes in general [Ph.D. thesis]: Los Angeles, California, USA, University of California–Los Angeles, 292 p.

Guest, B., Axen, G.J., Hassanzadeh, J., Cummings, D., and McIntosh, W., 2001, Preliminary sedimentary-tectonic history and Ar/Ar ages from the "Neogene" redbeds, Taleghan Valley, Alborz Mountains, Iran: Geological Society of America Abstracts with Programs, v. 33, no. 6, p. 258–259.

Hassanzadeh, J., Ghazi, A.M., Axen, G., and Guest, B., 2002, Oligo-Miocene mafic-alkaline magmatism in north and northwest of Iran: Evidence for the separation of the Alborz from the Urumieh-Dokhtar magmatic arc: Geological Society of America Abstracts with Programs, v. 34, no. 6, p. 331.

Huber, H., and Eftekhar-nezhad, J., 1978a, Geological map of Iran, sheet no. 1, northwest Iran: Tehran, National Iranian Oil Company, scale 1:1,000,000.

Huber, H., and Eftekhar-nezhad, J., 1978b, Geological map of Iran, sheet no. 2, north-central Iran: Tehran, National Iranian Oil Company, scale 1:1,000,000.

Jackson, J., Priestley, K., Allen, M., and Berberian, M., 2002, Active tectonics of the South Caspian Basin: Geophysical Journal International, v. 148, p. 214–245, doi: 10.1046/j.1365-246X.2002.01588.x.

Lam, P.J., 2002, Geology, geochronology, and thermochronology of the Alam Kuh area, central Alborz Mountains northern Iran [M.S. thesis]: Los Angeles, California, University of California–Los Angeles, 135 p.

Lyberis, N., and Manby, G., 1999, Oblique and orthogonal convergence across the Turan block in the post-Miocene: American Association of Petroleum Geologists Bulletin, v. 83, p. 1135–1160.

McQuarrie, N., 2004, Crustal scale geometry of the Zagros fold-thrust belt, Iran: Journal of Structural Geology, v. 26, p. 519–535, doi: 10.1016/j.jsg.2003.08.009.

McQuarrie, N., Stock, J.M., Verdel, C., and Wernicke, B.P., 2003, Cenozoic evolution of Neotethys and implications for the causes of plate motions: Geophysical Research Letters, v. 30, no. 20, 2036, doi: 10.1029/2003GL017992.

Mohajjel, M., Fergusson, C.L., and Sahandi, M.R., 2003, Cretaceous-Tertiary convergence and continental collision, Sanandaj-Sirjan zone, western Iran: Journal of Asian Earth Sciences, v. 21, p. 397–412, doi: 10.1016/S1367-9120(02)00035-4.

Nilforoushan, F., Masson, F., Vernant, P., Vigny, C., Martinod, J., Abbassi, M., Nankali, H., Hatzfeld, D., Bayer, R., Tavakoli, F., Ashtiani, A., Doerflinger, E., Daignieres, M., Collard, P., and Chery, J., 2003, GPS network monitors the Arabia-Eurasia collision deformation in Iran: Journal of Geodesy, v. 77, p. 411–422, doi: 10.1007/s00190-003-0326-5.

Ritz, J.-F., Balescu, S., Soleymani, S., Abbassi, M., Nazari, H., Feghhi, K., Shabanian, E., Tabassi, H., Farbod, Y., Lamothe, M., Michelot, J.-L., Chery, J., and Vernant, P., 2003, Geometry, kinematics and slip rate along the Mosha active fault, central Alborz: Katlenburg-Lindau, Germany, European Geosciences Union, v, 5. European Geophysical Society–American Geophysical Union–European Union of Geophysicists Joint Assembly, Nice, France, Abstract EAE03-A-06057.

Şengör, A.M.C., 1990, A new model for the late Paleozoic-Mesozoic tectonic evolution of Iran and implications for Oman, *in* Searle, M.P., and Ries, A.C., eds., The geology and tectonics of the Oman region: London, Geological Society [London], p. 797–831.

Şengör, A.M.C., and Kidd, W.S.F., 1979, Post-collisional tectonics of the Turkish-Iranian plateau and a comparison with Tibet: Tectonophysics, v. 55, p. 361–376, doi: 10.1016/0040-1951(79)90184-7.

Şengör, A.M.C., and Natal'in, B.A., 1996, Paleotectonics of Asia: Fragments of a synthesis, *in* Yin, A., and Harrison, M., eds., The tectonic evolution of Asia: Cambridge, Cambridge University Press, p. 486–640.

Şengör, A.M.C., Altiner, D., Cin, A., Ustaomer, T., and Hsu, K.J., 1988, Origin and assembly of the Tethyside orogenic collage at the expense of Gondwana Land, in Audley-Charles, M.G., and Hallman, A., eds., Gondwana and Tethys: Geological Society [London] Special Publication 37, p. 119–181.

Sieber, N., 1970, Zur Geologie des Gebietes sudlich des Taleghan-Tales Zentral Elburz (Iran) [Ph.D. thesis]: Zürich, Eidgenössische Technische Hochschule, 126 p.

Stampfli, G.M., Marcoux, J., and Baud, A., 1991, Tethyan margins in space and time: Palaeogeography, Palaeoclimatology, Palaeoecology, v. 87, p. 373–409, doi: 10.1016/0031-0182(91)90142-E.

Stocklin, J., 1974a, Northern Iran: Alborz Mountains, *in* Spencer, A.M., ed., Mesozoic-Cenozoic orogenic belts; data for orogenic studies; Alpine-Himalayan orogens: Geological Society [London] Special Publication 4, p. 213–234.

Stocklin, J., 1974b, Possible ancient continental margins in Iran, *in* Burke, C., and Drake, C., eds., The geology of continental margins: Berlin, Springer-Verlag, p. 873–887.

Stocklin, J., and Setudehnia, A., 1977, Stratigraphic lexicon of Iran: Tehran, Geological Survey of Iran, 409 p.

Taylor, M., Yin, A., Ryerson, F.J., Kapp, P., and Ding, L., 2003, Conjugate strike-slip faulting along the Bangong-Nujiang suture zone accommodates coeval east-west extension and north-south shortening in the interior of the Tibetan Plateau: Tectonics, v. 22, no. 4, p. 18-1–18-16.

Vahdati Daneshmand, F., 1991, Amol: Geological quadrangle map of Iran: Tehran, Geological Survey of Iran, scale 1:250,000.

Vernant, P., Nilforoushan, F., Chery, J., Bayer, R., Djamour, Y., Masson, F., Nankali, H., Ritz, J.-F., Sedighi, M., and Tavakoli, F., 2004, Deciphering oblique shortening of central Alborz in Iran using geodetic data: Earth and Planetary Science Letters, v. 223, p. 177–185, doi: 10.1016/j.epsl.2004.04.017.

Woodruff, F., and Savin, S.M., 1989, Miocene deepwater oceanography: Paleoceanography, v. 4, p. 87–140.

Yilmaz, Y., 1993, New evidence and model on the evolution of the southeast Anatolian orogen: Geological Society of America Bulletin, v. 105, p. 251–271, doi: 10.1130/0016-7606(1993)105<0251:NEAMOT>2.3.CO;2.

Manuscript Received by the Society 20 April 2005
Revised Manuscript Received 28 November 2005
Manuscript Accepted 29 November 2005

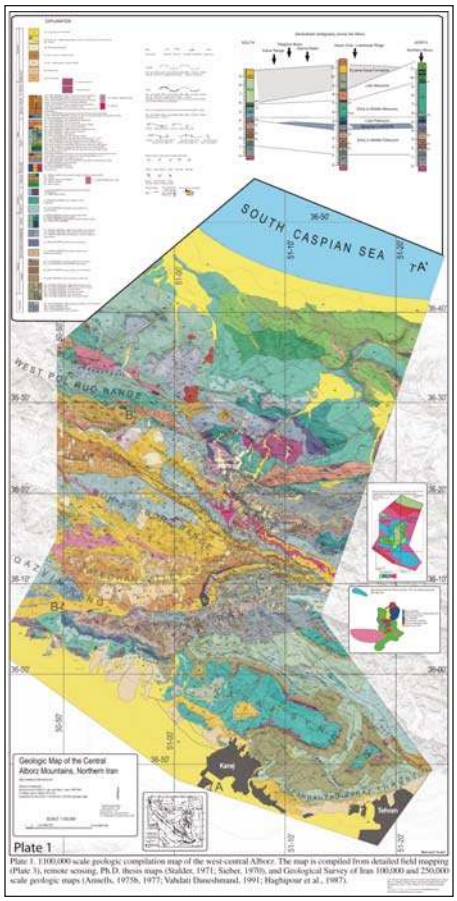

Plate 1. 1:100,000 scale geologic compilation map of the west-central Alborz. The map is compiled from detailed field mapping (Plate 3), remote sensing, Ph.D. thesis maps (Stalder, 1971; Sieber, 1970), and Geological Survey of Iran 100,000 and 250,000 scale geologic maps (Annells, 1975b, 1977; Vahdati Daneshmand, 1991; Haghipour et al., 1987). If you are viewing the PDF, or if you are reading this offline, please visit the full-text version of this article at www.gsajournals.org or http://dx.doi.org/10.1130/GES00019.PL1 to view the plate.

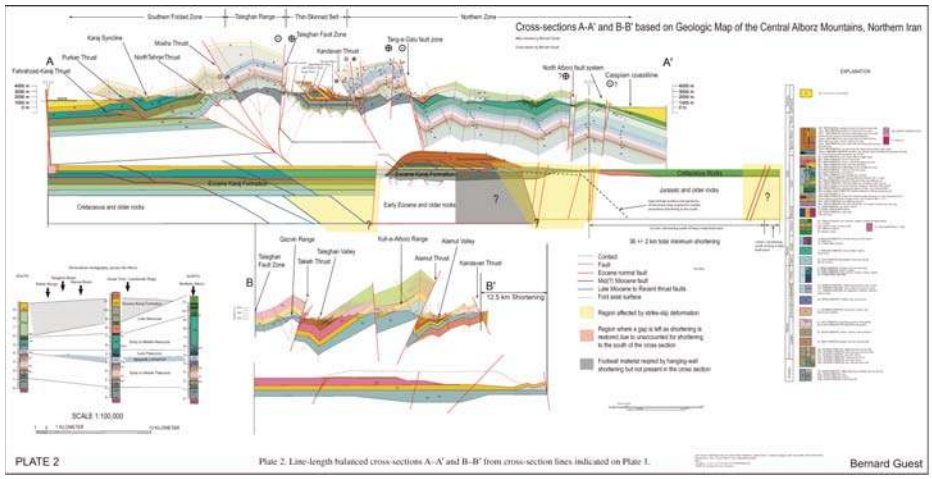

Plate 2. Line-length balanced cross-sections A–A′ and B–B′ from cross-section lines indicated on Plate 1. If you are viewing the PDF, or if you are reading this offline, please visit the full-text version of this article at www.gsajournals.org or http://dx.doi.org/10.1130/GES00019.PL2 to view the plate.

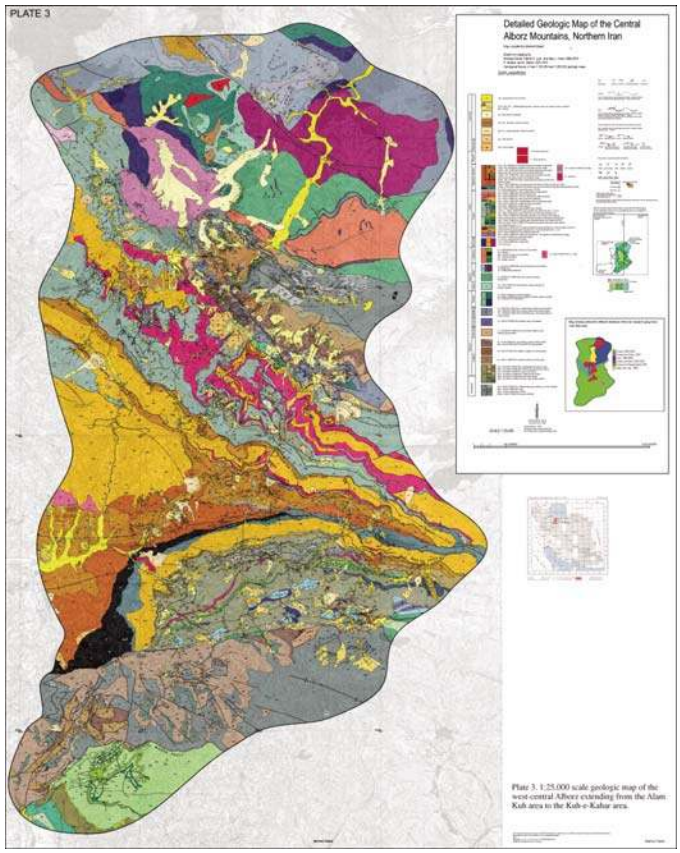

Plate 3. 1:25,000 scale geologic map of the west-central Alborz extending from the Alam Kuh area to the Kuh-e-Kahar area. If you are viewing the PDF, or if you are reading this offline, please visit the full-text version of this article at www.gsajournals.org or http://dx.doi.org/10.1130/GES00019.PL3 to view the plate.